

NLO contributions to $B \rightarrow KK^*$ Decays in the pQCD approach

Zhi-Qing Zhang ^{*} and Zhen-Jun Xiao [†]

*Department of Physics and Institute of Theoretical Physics,
Nanjing Normal University, Nanjing, Jiangsu 210097, P.R.China [‡]*

(Dated: October 31, 2018)

Abstract

We calculate the important next-to-leading-order (NLO) contributions to the $B \rightarrow KK^*$ decays from the vertex corrections, the quark loops, and the magnetic penguins in the perturbative QCD (pQCD) factorization approach. The pQCD predictions for the CP-averaged branching ratios are $Br(B^+ \rightarrow K^+\bar{K}^{*0}) \approx 3.2 \times 10^{-7}$, $Br(B^+ \rightarrow \bar{K}^0 K^{*+}) \approx 2.1 \times 10^{-7}$, $Br(B^0/\bar{B}^0 \rightarrow K^0\bar{K}^{*0} + \bar{K}^0 K^{*0}) \approx 8.5 \times 10^{-7}$, $Br(B^0/\bar{B}^0 \rightarrow K^+K^{*-} + K^-K^{*+}) \approx 1.3 \times 10^{-7}$, which agree well with both the experimental upper limits and the predictions based on the QCD factorization approach. Furthermore, the CP-violating asymmetries of the considered decay modes are also evaluated. The NLO pQCD predictions for $\mathcal{A}_{CP}(B^+ \rightarrow K^+\bar{K}^{*0})$ and $\mathcal{A}_{CP}(B^+ \rightarrow K^{*+}\bar{K}^0)$ are $\mathcal{A}_{CP}^{dir}(K^+\bar{K}^{*0}) \approx -6.9\%$ and $\mathcal{A}_{CP}^{dir}(K^{*+}\bar{K}^0) \approx 6.5\%$.

PACS numbers: 13.25.Hw, 12.38.Bx, 14.40.Nd

arXiv:0807.2022v1 [hep-ph] 13 Jul 2008

^{*} Electronic address: zhangzhiqing@zzu.edu.cn

[†] Electronic address: xiaozhenjun@njnu.edu.cn

[‡] Mailing address

I. INTRODUCTION

It is well-known that the experimental measurements and theoretical studies of the two body charmless hadronic B meson decays play an important role in the precision test of the standard model (SM) and in searching for the new physics beyond the SM [1]. For these decays, the dominant theoretical error comes from the large uncertainty in evaluating the so-called hadronic matrix element, $\langle M_1 M_2 | O_i | B \rangle$, where M_1 and M_2 are light final state mesons. The perturbative QCD (pQCD) approach [2] is one of the most popular factorization approaches [3, 4] being used to calculate the hadronic matrix elements.

When compared with the QCDF or SCET factorization approaches, the pQCD approach has the following three special features: (a) since the k_T factorization is employed here, the resultant Sudakov factor as well as the threshold resummation can enable us to regulate the end-point singularities effectively; (b) the form factors for $B \rightarrow M$ transition can be calculated perturbatively, although some controversies still exist about this point; and (c) the annihilation diagrams are calculable and play an important role in producing CP violation.

Up to now, almost all two-body charmless $B/B_s \rightarrow M_1 M_2$ decays have been calculated by using the pQCD approach at the leading order [5, 6, 7, 8, 9, 10, 11, 12]. Very recently, some next-to-leading (NLO) contributions to $B \rightarrow K\pi$ and several $B \rightarrow PV$ decay modes [13, 14] have been calculated, where the Wilson coefficients at NLO accuracy are used, and the contributions from the vertex corrections, the quark loops and the chromo-magnetic penguin operator O_{8g} have been taken into account. As generally expected, the inclusion of NLO contributions should improve the reliability of the pQCD predictions.

In a previous paper [10], the authors calculated the branching ratios and CP violating asymmetries of the $B^0/\overline{B}^0 \rightarrow K^0\overline{K}^{*0}, \overline{K}^0 K^{*0}, K^+ K^{*-}, K^- K^{*+}$, and $B^+ \rightarrow K^+\overline{K}^{*0}$ and $\overline{K}^0 K^{*+}$ decays by employing the pQCD approach at the leading order. Following the procedure of Ref. [13], we here would like to calculate the NLO contributions to the $B \rightarrow K^* K$ decays by employing the low energy effective Hamiltonian and the pQCD approach.

The remainder of the paper is organized as follows. In Sec.II, we give a brief discussion about pQCD factorization approach. In Sec. III, we calculate analytically the relevant Feynman diagrams and present the various decay amplitudes for the studied decay modes in leading-order. In Sec. IV, the NLO contributions from the vertex corrections, the quark loops and the chromo-magnetic penguin amplitudes are evaluated. We show the numerical results for the branching ratios and CP asymmetries of $B \rightarrow K^* K$ decays in Sec. V. The summary and some discussions are included in the final section.

II. THEORETICAL FRAMEWORK

The pQCD factorization approach has been developed and applied in the non-leptonic B meson decays [2] for some time. In this approach, the decay amplitude is separated into soft, hard, and harder dynamics characterized by different energy scales (t, m_b, M_W).

It is conceptually written as the convolution,

$$\mathcal{A}(B \rightarrow M_1 M_2) \sim \int d^4 k_1 d^4 k_2 d^4 k_3 \text{Tr} [C(t) \Phi_B(k_1) \Phi_{M_1}(k_2) \Phi_{M_2}(k_3) H(k_1, k_2, k_3, t)], \quad (1)$$

where k_i 's are momenta of light quarks included in each meson, and Tr denotes the trace over Dirac and color indices. $C(t)$ is the Wilson coefficient, which includes the harder dynamics at larger scale than M_B scale and describes the evolution of local 4-Fermi operators from m_W down to $t \sim \mathcal{O}(\sqrt{\bar{\Lambda} M_B})$ scale, where $\bar{\Lambda} \equiv M_B - m_b$. The function $H(k_1, k_2, k_3, t)$ describes the four quark operator and the spectator quark connected by a hard gluon whose q^2 is in the order of $\bar{\Lambda} M_B$, and includes the $\mathcal{O}(\sqrt{\bar{\Lambda} M_B})$ hard dynamics. Therefore, this hard part H can be perturbatively calculated. The function Φ_{M_i} is the wave function which describes hadronization of the quark and anti-quark into the meson M_i . While the function H depends on the processes considered, the wave function Φ_{M_i} is independent of the specific processes.

In the B meson rest-frame, it is convenient to use light-cone coordinate (p^+, p^-, \mathbf{p}_T) to describe the meson's momenta,

$$p^\pm = \frac{1}{\sqrt{2}}(p^0 \pm p^3), \quad \text{and} \quad \mathbf{p}_T = (p^1, p^2). \quad (2)$$

Using these coordinates the B meson and the two final state meson momenta can be written as

$$P_B = \frac{M_B}{\sqrt{2}}(1, 1, \mathbf{0}_T), \quad P_{K^*} = \frac{M_B}{\sqrt{2}}(1, r_{K^*}^2, \mathbf{0}_T), \quad P_K = \frac{M_B}{\sqrt{2}}(0, 1 - r_{K^*}^2, \mathbf{0}_T), \quad (3)$$

respectively, here $r_{K^*} = m_{K^*}/M_B$. The light meson (K) mass has been neglected. For the $B \rightarrow K^* K$ decays considered here, only the vector meson's longitudinal part contributes to the decays, and its polarization vector is $\epsilon_L = \frac{M_B}{\sqrt{2}M_{K^*}}(1, -r_{K^*}^2, 0_T)$. Putting the anti-quark momenta in B , K^* and K mesons as k_1 , k_2 , and k_3 , respectively, we can choose

$$k_1 = (x_1 P_1^+, 0, \mathbf{k}_{1T}), \quad k_2 = (x_2 P_2^+, 0, \mathbf{k}_{2T}), \quad k_3 = (0, x_3 P_3^-, \mathbf{k}_{3T}). \quad (4)$$

Then, the integration over $k_1^-, k_2^-,$ and k_3^+ in eq.(1) will lead to

$$\mathcal{A}(B \rightarrow K K^*) \sim \int dx_1 dx_2 dx_3 b_1 db_1 b_2 db_2 b_3 db_3 \cdot \text{Tr} [C(t) \Phi_B(x_1, b_1) \Phi_{K^*}(x_2, b_2) \Phi_K(x_3, b_3) H(x_i, b_i, t) S_t(x_i) e^{-S(t)}], \quad (5)$$

where b_i is the conjugate space coordinate of k_{iT} , and t is the largest energy scale in function $H(x_i, b_i, t)$. The large logarithms ($\ln m_W/t$) coming from QCD radiative corrections to four quark operators are included in the Wilson coefficients $C(t)$. The large double logarithms ($\ln^2 x_i$) on the longitudinal direction are summed by the threshold resummation [15], and they lead to $S_t(x_i)$ which smears the end-point singularities on x_i . The last term, $e^{-S(t)}$, is the Sudakov form factor which suppresses the soft dynamics effectively [2]. Thus it makes the perturbative calculation of the hard part H applicable at intermediate scale, i.e., M_B scale.

A. Wilson Coefficients

For $B \rightarrow KK^*$ decays, the related weak effective Hamiltonian H_{eff} with $b \rightarrow s$ transition can be written as [16]

$$\mathcal{H}_{eff} = \frac{G_F}{\sqrt{2}} \left\{ \sum_{q=u,c} V_{qb}V_{qs}^* [C_1(\mu)O_1^q(\mu) + C_2(\mu)O_2^q(\mu)] - V_{tb}V_{td}^* \sum_{i=3}^{10} C_i(\mu) O_i(\mu) \right\}. \quad (6)$$

with $G_F = 1.16639 \times 10^{-5} GeV^{-2}$ is the Fermi constant, and V_{ij} is the CKM matrix element, $C_i(\mu)$ are the Wilson coefficients evaluated at the renormalization scale μ and O_i are the four-fermion operators. For the case of $b \rightarrow d$ transition, simply make a replacement of s by d in Eq. (6) and in the expressions of O_i operators, which can be found easily for example in Refs.[10, 16].

In PQCD approach, the energy scale "t" is chosen at the maximum value of various subprocess scales to suppress the higher order corrections, which may be larger or smaller than the m_b scale. In the range of $t < m_b$ or $t \geq m_b$, the number of active quarks is $N_f = 4$ or $N_f = 5$, respectively. For the Wilson coefficients $C_i(\mu)$ and their renormalization group (RG) running, they are known at NLO level currently [16]. The explicit expressions of the LO and NLO $C_i(m_W)$ can be found easily, for example, in Refs. [6, 16].

When the pQCD approach at leading-order are employed, the leading order Wilson coefficients $C_i(m_W)$, the leading order RG evolution matrix $U(t, m)^{(0)}$ from the high scale m down to $t < m$ (for details see Eq. (3.94) in Ref. [16]), and the leading order $\alpha_s(t)$ are used:

$$\alpha_s(t) = \frac{4\pi}{\beta_0 \ln [t^2/\Lambda_{QCD}^2]}, \quad (7)$$

where $\beta_0 = (33 - 2N_f)/3$, $\Lambda_{QCD}^{(5)} = 0.225 GeV$ and $\Lambda_{QCD}^{(4)} = 0.287 GeV$.

When the NLO contributions are taken into account, however, the NLO Wilson coefficients $C_i(m_W)$, the NLO RG evolution matrix $U(t, m, \alpha)$ (for details see Eq. (7.22) in Ref. [16]) and the $\alpha_s(t)$ at two-loop level are used:

$$\alpha_s(t) = \frac{4\pi}{\beta_0 \ln [t^2/\Lambda_{QCD}^2]} \cdot \left\{ 1 - \frac{\beta_1}{\beta_0^2} \cdot \frac{\ln [\ln [t^2/\Lambda_{QCD}^2]]}{\ln [t^2/\Lambda_{QCD}^2]} \right\}, \quad (8)$$

where $\beta_0 = (33 - 2N_f)/3$, $\beta_1 = (306 - 38N_f)/3$, $\Lambda_{QCD}^{(5)} = 0.225 GeV$ and $\Lambda_{QCD}^{(4)} = 0.326 GeV$.

By using the input parameters as given in the Appendix, it is easy to find the numerical values of the LO and NLO Wilson coefficients $C_i(m_b)$ for $m_b = 4.8 GeV$, as listed in Table I.

B. Wave Functions

The B meson is treated as a heavy-light system. For the B meson wave function, since the contribution of $\bar{\phi}_B$ is numerically small [17], we here only consider the contribution

TABLE I: The numerical values of the LO and NLO Wilson coefficients $C_i(m_b)$, $C_{7\gamma}(m_b)$ and $C_{8g}(m_b)$.

$C_i(m_b)$	C_1	C_2	C_3	C_4	C_5	C_6
LO	-0.2812	1.1246	0.0130	-0.0278	0.0080	-0.0343
NLO	-0.1747	1.0774	0.0125	-0.0330	0.0094	-0.0393
$C_i(m_b)$	C_7/α	C_8/α	C_9/α	C_{10}/α	$C_{7\gamma}$	C_{8g}
LO	0.1338	0.0514	-1.1459	0.2865	-0.3109	-0.1481
NLO	-0.0032	0.0305	-1.2760	0.2553	-0.3016	--

of Lorentz structure

$$\Phi_B = \frac{1}{\sqrt{2N_c}}(\not{p}_B + m_B)\gamma_5\phi_B(\mathbf{k}_1), \quad (9)$$

with

$$\phi_B(x, b) = N_B x^2 (1-x)^2 \exp\left[-\frac{M_B^2 x^2}{2\omega_b^2} - \frac{1}{2}(\omega_b b)^2\right], \quad (10)$$

where ω_b is a free parameter and we take $\omega_b = 0.4 \pm 0.04$ GeV in numerical calculations, and $N_B = 101.445$ is the normalization factor for $\omega_b = 0.4$.

The K and K^* mesons are all treated as a light-light system. The wave function of K meson is defined as [18]

$$\Phi_K(P, x, \zeta) \equiv \frac{1}{\sqrt{2N_C}}\gamma_5 [\not{p}\phi_K^A(x) + m_0^K \phi_K^P(x) + \zeta m_0^K (\not{p}\not{\eta} - v \cdot n)\phi_K^T(x)], \quad (11)$$

where P and x are the momentum and the momentum fraction of K , respectively. The parameter ζ is either +1 or -1 depending on the assignment of the momentum fraction x . For the considered $B \rightarrow KK^*$ decays, K^* meson is longitudinally polarized, and only the longitudinal component $\phi_{K^*}^L$ of the wave function contribute [18]

$$\phi_{K^*}^L = \frac{1}{\sqrt{2N_c}} \{ \not{\epsilon}_L [m_{K^*}\phi_{K^*}(x) + \not{p}_{K^*}\phi_{K^*}^t(x)] + m_{K^*}\phi_{K^*}^s(x) \}, \quad (12)$$

where the first term is the leading twist wave function (twist-2), while the second and third term are sub-leading twist (twist-3) wave functions.

The expressions of the relevant distributions functions are the following [18]:

$$\phi_K^A(x) = \frac{f_K}{2\sqrt{2N_c}} 6x(1-x) \left[1 + a_1^K C_1^{3/2}(t) + a_2^K C_2^{3/2}(t) + a_4^K C_4^{3/2}(t) \right], \quad (13)$$

$$\phi_K^P(x) = \frac{f_K}{2\sqrt{2N_c}} \left[1 + (30\eta_3 - \frac{5}{2}\rho_K^2)C_2^{1/2}(t) - 3 \left[\eta_3\omega_3 + \frac{9}{20}\rho_K^2(1 + 6a_2^K) \right] C_4^{1/2}(t) \right], \quad (14)$$

$$\phi_K^T(x) = -\frac{f_K}{2\sqrt{2N_c}} t \left[1 + 6(5\eta_3 - \frac{1}{2}\eta_3\omega_3 - \frac{7}{20}\rho_K^2 - \frac{3}{5}\rho_K^2 a_2^K)(1 - 10x + 10x^2) \right], \quad (15)$$

with the mass ratio $\rho_K = m_K/m_{0K}$, and $\eta_3 = 0.015$, $\omega = -3.0$. Since the uncertainties of the currently available Gegenbauer moments [19] are still large, we vary the value of a_K^1 and a_K^4 by 100%, i.e. $a_1^K = 0.17 \pm 0.17$, $a_2^K = 0.115 \pm 0.115$, but keep $a_4^K = -0.015$, because the theoretical predictions are insensitive to a_K^4 .

The twist-2 DAs for longitudinally polarized vector meson K^* can be parameterized as:

$$\phi_{K^*}(x) = \frac{f_{K^*}}{2\sqrt{2N_c}} 6x(1-x) \left[1 + a_{1K^*} C_1^{3/2}(t) + a_{2K^*} C_2^{3/2}(t) \right], \quad (16)$$

where $f_{K^*} = 200$ MeV is the decay constant of the vector meson with longitudinal polarization, and the Gegenbauer moments are $a_{1K^*} = 0.03 \pm 0.03$, $a_{2K^*} = 0.11 \pm 0.11$. As for the twist-3 DAs $\phi_{K^*}^s$ and $\phi_{K^*}^t$, there is no recent update associated with those updates for twist-2 DAs, we adopt their asymptotic form:

$$\phi_{K^*}^s(x) = \frac{3f_{K^*}^T}{2\sqrt{2N_c}}(1-2x), \quad \phi_{K^*}^t(x) = \frac{3f_{K^*}^T}{2\sqrt{2N_c}}(2x-1)^2, \quad (17)$$

At last the Gegenbauer polynomials $C_n^\nu(t)$ are given as:

$$\begin{aligned} C_2^{1/2}(t) &= \frac{1}{2}(3t^2 - 1), & C_4^{1/2}(t) &= \frac{1}{8}(3 - 30t^2 + 35t^4), \\ C_1^{3/2}(t) &= 3t, & C_2^{3/2}(t) &= \frac{3}{2}(5t^2 - 1), \\ C_4^{3/2}(t) &= \frac{15}{8}(1 - 14t^2 + 21t^4), \end{aligned} \quad (18)$$

with $t = 2x - 1$.

III. DECAY AMPLITUDES AT LEADING ORDER IN PQCD APPROACH

The $B \rightarrow KK^*$ decays have been studied previously in Ref. [10] by using the leading order pQCD approach. In this paper, we focus on the calculations of some NLO contributions to these decays in the pQCD factorization approach. For the sake of completeness, however, we firstly recalculate and present the relevant LO decay amplitudes in this section.

At the leading order, the relevant Feynman diagrams for $B^0 \rightarrow K^{*0}\bar{K}^0$, $K^0\bar{K}^{*0}$, $B^0 \rightarrow K^+K^{*-}$, K^-K^{*+} , and $B^+ \rightarrow K^+\bar{K}^{*0}$, $K^{*+}\bar{K}^0$ decays have been shown in Figs. 1, 2 and 3.

As illustrated by Fig. 1, both B^0 and \bar{B}^0 can decay into $K^{*0}\bar{K}^0$ and $K^0\bar{K}^{*0}$ simultaneously. Besides of the eight Feynman diagrams in Fig. 1, other four Feynman diagrams can be obtained by connecting the left-hand end of the gluon line to the lower d quark line inside the B^0 meson for (e) and (f), or to the lower s or d quark line for (g) and (h). For $B^0 \rightarrow K^{*0}\bar{K}^0$ and $K^0\bar{K}^{*0}$ decays, only the operators O_{3-10} contribute via penguin topology. Its is a pure penguin mode with only one kind of CKM element $\xi_t = V_{tb}^*V_{td}$, and therefore there is no CP violation for such decays at leading order.

For $B^0 \rightarrow K^{*0}\bar{K}^0$, $K^0\bar{K}^{*0}$ decays, we firstly consider the case of $B \rightarrow K^{*0}$ transition where K^{*0} meson takes the spectator d quark. For the $(V-A)(V-A)$ operators, the

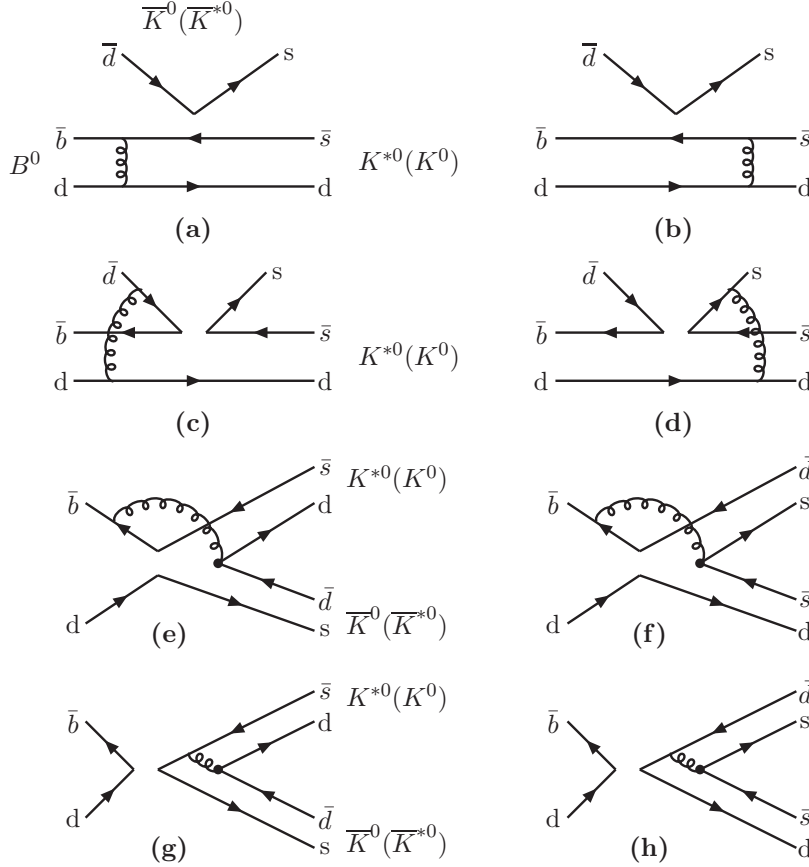


FIG. 1: Diagrams contributing to the $B^0 \rightarrow K^{*0} \bar{K}^0$ decay. From diagram (a) and (b), the form factor $A_0^{B \rightarrow K^*}$ or $F_{0,1}^{B \rightarrow K}$ can be extracted. Other four Feynman diagrams can be obtained by connecting the left-hand end of the gluon line to lower d quark line inside the B^0 meson for (e) and (f), while to the lower s or d quark line for (g) and (h).

decay amplitude corresponding to Figs. (1)a and (1)b can be written as

$$\begin{aligned}
F_{eK^*} &= 4\sqrt{2}G_F\pi C_F f_K m_B^4 \int_0^1 dx_1 dx_2 \int_0^\infty b_1 db_1 b_2 db_2 \phi_B(x_1, b_1) \\
&\times \left\{ \left[(1+x_2)\phi_{K^*}(\bar{x}_2) - (1-2x_2)r_{K^*}(\phi_{K^*}^s(\bar{x}_2) - \phi_{K^*}^t(\bar{x}_2)) \right] \right. \\
&\left. \cdot E_e(t_a) h_e(x_1, x_2, b_1, b_2) - 2r_{K^*}\phi_{K^*}^s(\bar{x}_2) \cdot E_e(t'_a) h_e(x_2, x_1, b_2, b_1) \right\}, \quad (19)
\end{aligned}$$

where $r_{K^*} = m_{K^*}/m_B$, $C_F = 4/3$ is a color factor. The evolution factors $E_e(t_a^{(l)})$ and the hard functions h_e are displayed in Appendix A.

For the $(V-A)(V+A)$ and $(S-P)(S+P)$ operators, we find

$$F_{eK^*}^{P1} = -F_{eK^*}, \quad (20)$$

$$\begin{aligned}
F_{eK^*}^{P2} &= 8\sqrt{2}G_F\pi C_F f_K m_B^4 \int_0^1 dx_1 dx_2 \int_0^\infty b_1 db_1 b_2 db_2 \phi_B(x_1) \\
&\times \left\{ -r_K \left[\phi_{K^*}(\bar{x}_2) - r_{K^*}((2+x_2)\phi_{K^*}^s(\bar{x}_2) + x_2\phi_{K^*}^t(\bar{x}_2)) \right] \right. \\
&\left. \cdot E_e(t_a) h_e(x_1, x_2, b_1, b_2) + 2r_{K^*}r_K\phi_{K^*}^s(\bar{x}_2) \cdot E_e(t'_a) h_e(x_2, x_1, b_2, b_1) \right\}. \quad (21)
\end{aligned}$$

For the non-factorizable diagrams 1(c) and 1(d), all three meson wave functions are

involved. The decay amplitudes are

$$\begin{aligned}
M_{eK^*} &= \frac{16}{\sqrt{3}} G_F \pi C_F m_B^4 \int_0^1 dx_1 dx_2 dx_3 \int_0^\infty b_1 db_1 b_3 db_3 \phi_B(x_1, b_1) \phi_K^A(\bar{x}_3) \\
&\times \left\{ [r_{K^*} x_2 (\phi_{K^*}^s(\bar{x}_2) + \phi_{K^*}^t(\bar{x}_2)) + (1 - x_3) \phi_{K^*}(\bar{x}_2)] \right. \\
&\cdot E'_e(t_b) h_n(x_1, x_2, 1 - x_3, b_1, b_3) + E'_e(t'_b) h_n(x_1, x_2, x_3, b_1, b_3) \\
&\cdot \left. [-(x_2 + x_3) \phi_{K^*}(\bar{x}_2) - r_{K^*} x_2 (\phi_{K^*}^s(\bar{x}_2) - \phi_{K^*}^t(\bar{x}_3))] \right\}, \tag{22}
\end{aligned}$$

$$\begin{aligned}
M_{eK^*}^{P1} &= -\frac{16}{\sqrt{3}} G_F \pi C_F m_B^4 r_K \int_0^1 dx_1 dx_2 dx_3 \int_0^\infty b_1 db_1 b_3 db_3 \phi_B(x_1, b_1) \times \{ [(1 - x_3) \phi_{K^*}(\bar{x}_2) \\
&\cdot (\phi_K^P(\bar{x}_3) - \phi_K^T(\bar{x}_3)) - r_{K^*} (1 - x_3) (\phi_{K^*}^s(\bar{x}_2) + \phi_{K^*}^t(\bar{x}_2)) (\phi_K^P(\bar{x}_3) - \phi_K^T(\bar{x}_3)) \\
&- r_{K^*} x_2 (\phi_{K^*}^s(\bar{x}_2) - \phi_{K^*}^t(\bar{x}_2)) (\phi_K^P(\bar{x}_3) + \phi_K^T(\bar{x}_3))] E'_e(t_b) h_n(x_1, x_2, 1 - x_3, b_1, b_3) \\
&- [x_3 \cdot \phi_{K^*}(\bar{x}_2) (\phi_K^P(\bar{x}_3) + \phi_K^T(\bar{x}_3)) - r_{K^*} x_3 (\phi_{K^*}^s(\bar{x}_2) + \phi_{K^*}^t(\bar{x}_2)) (\phi_K^P(\bar{x}_3) \\
&+ \phi_K^T(\bar{x}_3)) - r_{K^*} x_2 (\phi_{K^*}^s(\bar{x}_2) - \phi_{K^*}^t(\bar{x}_2)) (\phi_K^P(\bar{x}_3) - \phi_K^T(\bar{x}_3))] \\
&\times E'_e(t'_b) h_n(x_1, x_2, x_3, b_1, b_3) \}, \tag{23}
\end{aligned}$$

$$M_{eK^*}^{P2} = 0. \tag{24}$$

For the non-factorizable annihilation diagrams (e) and (f), again all three wave functions are involved. The decay amplitudes are

$$\begin{aligned}
M_{aK^*} &= \frac{16}{\sqrt{3}} G_F \pi C_F m_B^4 \int_0^1 dx_1 dx_2 dx_3 \int_0^\infty b_1 db_1 b_3 db_3 \phi_B(x_1, b_1) \\
&\times \left\{ [(1 - x_2) \phi_{K^*}(\bar{x}_2) \phi_K^A(\bar{x}_3) + r_{K^*} r_K (1 - x_2) (\phi_{K^*}^s(\bar{x}_2) + \phi_{K^*}^t(\bar{x}_2)) (\phi_K^P(\bar{x}_3) - \right. \\
&\phi_K^T(\bar{x}_3)) + r_{K^*} r_K x_3 (\phi_{K^*}^s(\bar{x}_2) - \phi_{K^*}^t(\bar{x}_2)) (\phi_K^P(\bar{x}_3) + \phi_K^T(\bar{x}_3))] \\
&\times E'_a(t_c) h_{na}(x_1, x_2, x_3, b_1, b_3) - E'_a(t'_c) h'_{na}(x_1, x_2, x_3, b_1, b_3) [x_3 \phi_{K^*}(\bar{x}_2) \phi_K^A(\bar{x}_3) \\
&+ 4r_{K^*} r_K \phi_{K^*}^s(\bar{x}_2) \phi_K^P(\bar{x}_3) - r_{K^*} r_K (1 - x_3) (\phi_{K^*}^s(\bar{x}_2) + \phi_{K^*}^t(\bar{x}_2)) (\phi_K^P(\bar{x}_3) \\
&- \phi_K^T(\bar{x}_3)) - r_{K^*} r_K x_2 (\phi_{K^*}^s(\bar{x}_2) - \phi_{K^*}^t(\bar{x}_2)) (\phi_K^P(\bar{x}_3) + \phi_K^T(\bar{x}_3))] \}, \tag{25}
\end{aligned}$$

$$\begin{aligned}
M_{aK^*}^{P1} &= \frac{16}{\sqrt{3}} G_F \pi C_F m_B^4 \int_0^1 dx_1 dx_2 dx_3 \int_0^\infty b_1 db_1 b_3 db_3 \phi_B(x_1, b_1) \\
&\{ [(1 - x_2) r_{K^*} \phi_K^A(\bar{x}_3) (\phi_{K^*}^s(\bar{x}_2) + \phi_{K^*}^t(\bar{x}_2)) - r_K x_3 \phi_{K^*}(\bar{x}_2) (\phi_K^P(\bar{x}_3) - \phi_K^T(\bar{x}_3))] \\
&\times E'_a(t_c) h_{na}(x_1, x_2, x_3, b_1, b_3) - [-(x_2 + 1) r_{K^*} \phi_K^A(\bar{x}_3) (\phi_{K^*}^s(\bar{x}_2) + \phi_{K^*}^t(\bar{x}_2)) \\
&- r_K (x_3 - 2) \phi_{K^*}(\bar{x}_2) (\phi_K^P(\bar{x}_3) - \phi_K^T(\bar{x}_3))] E'_a(t'_c) h'_{na}(x_1, x_2, x_3, b_1, b_3) \}. \tag{26}
\end{aligned}$$

$$\begin{aligned}
M_{aK^*}^{P2} &= \frac{16}{\sqrt{3}} G_F \pi C_F m_B^4 \int_0^1 dx_1 dx_2 dx_3 \int_0^\infty b_1 db_1 b_3 db_3 \phi_B(x_1, b_1) \{ [(x_2 - 1) \\
&\times \phi_{K^*}(\bar{x}_2) \phi_K^A(\bar{x}_3) - 4r_K r_{K^*} \phi_{K^*}^s(\bar{x}_2) \phi_K^P(\bar{x}_3) + r_K r_{K^*} x_2 (\phi_{K^*}^s(\bar{x}_2) + \phi_{K^*}^t(\bar{x}_2)) \\
&\cdot (\phi_K^P(\bar{x}_3) - \phi_K^T(\bar{x}_3)) + r_{K^*} r_K (1 - x_3) (\phi_{K^*}^s(\bar{x}_2) - \phi_{K^*}^t(\bar{x}_2)) (\phi_K^P(\bar{x}_3) + \phi_K^T(\bar{x}_3))] \\
&\cdot E'_a(t_e) h_{na}(x_1, x_2, x_3, b_1, b_3) + [x_3 \phi_{K^*}(\bar{x}_2) \phi_K^A(\bar{x}_3) + x_3 r_{K^*} r_K (\phi_{K^*}^s(\bar{x}_2) + \phi_{K^*}^t(\bar{x}_2)) \\
&\cdot (\phi_K^P(\bar{x}_3) - \phi_K^T(\bar{x}_3)) + r_{K^*} r_K (1 - x_2) (\phi_{K^*}^s(\bar{x}_2) - \phi_{K^*}^t(\bar{x}_2)) (\phi_K^P(\bar{x}_3) + \phi_K^T(\bar{x}_3))] \\
&\times E'_a(t'_e) h'_{na}(x_1, x_2, x_3, b_1, b_3) \}. \tag{27}
\end{aligned}$$

The factorizable annihilation diagrams (g) and (h) involve only K^* and K wave functions. There are also three kinds of decay amplitudes for these diagrams. F_{aK^*} is for $(V - A)(V - A)$

$$\begin{aligned}
F_{aK^*} = F_{aK^*}^{P1} = & 4\sqrt{2}G_F\pi C_F f_B m_B^4 \int_0^1 dx_2 dx_3 \int_0^\infty b_2 db_2 b_3 db_3 \{ - [(1 - x_2)\phi_{K^*}(\bar{x}_2) \\
& \cdot \phi_K^A(\bar{x}_3) + 4r_{K^*}r_{K^*}\phi_{K^*}^s(\bar{x}_2)\phi_K^P(\bar{x}_3) - 2r_{K^*}r_{K^*}x_2\phi_K^P(\bar{x}_3) (\phi_{K^*}^s(\bar{x}_2) + \phi_{K^*}^t(\bar{x}_2))] \\
& \cdot E_a(t_d)h_a(x_3, 1 - x_2, b_3, b_2) + [x_3\phi_{K^*}(\bar{x}_2)\phi_K^A(\bar{x}_3) + 2r_{K^*}r_{K^*}\phi_{K^*}^s(\bar{x}_2) \\
& \cdot (\phi_K^P(\bar{x}_3) + \phi_K^T(\bar{x}_3)) + 2r_{K^*}r_{K^*}x_3\phi_{K^*}^s(\bar{x}_2) (\phi_K^P(\bar{x}_3) - \phi_K^T(\bar{x}_3))] \\
& \times E_a(t'_d)h_a(1 - x_2, x_3, b_2, b_3) \} , \tag{28}
\end{aligned}$$

$$\begin{aligned}
F_{aK^*}^{P2} = & -8\sqrt{2}G_F\pi C_F f_B m_B^4 \int_0^1 dx_2 dx_3 \int_0^\infty b_2 db_2 b_3 db_3 \\
& \times \{ [r_{K^*}(1 - x_2) (\phi_{K^*}^s(\bar{x}_2) - \phi_{K^*}^t(\bar{x}_2)) \phi_K^A(\bar{x}_3) + 2r_{K^*}\phi_{K^*}(\bar{x}_2)\phi_K^P(\bar{x}_3)] \\
& \times E_a(t_d)h_a(x_3, 1 - x_2, b_3, b_2) \\
& + [2r_{K^*}\phi_{K^*}^s(\bar{x}_2)\phi_K^A(\bar{x}_3) + x_3r_{K^*}\phi_{K^*}(\bar{x}_2)(\phi_K^P(\bar{x}_3) + \phi_K^T(\bar{x}_3))] \\
& \times E_a(t'_d)h_a(1 - x_2, x_3, b_2, b_3) \} . \tag{29}
\end{aligned}$$

For the case of $B^0 \rightarrow K^0$ transition where K^0 meson takes up the spectator d quark, as shown in Fig. 1, it is straightforward to find the decay amplitudes by following the same procedure as the case of $B^0 \rightarrow K^{*0}$ transition.

$$\begin{aligned}
F_{eK} = & 16\pi C_F m_B^2 \int_0^1 dx_1 dx_2 \int_0^\infty b_1 db_1 b_2 db_2 \phi_B(x_1, b_1) \\
& \times \{ [(1 + x_2)\phi_K^A(\bar{x}_2) + (1 - 2x_2)r_K(\phi_K^P(\bar{x}_2) - \phi_K^T(\bar{x}_2))] E_e(t_a)h_e(x_1, x_2, b_1, b_2) \\
& + 2r_K\phi_K^P(\bar{x}_2)E_e(t'_a)h_e(x_2, x_1, b_2, b_1) \} , \tag{30}
\end{aligned}$$

$$F_{eK}^{P1} = F_{eK}, \quad F_{eK}^{P2} = 0. \tag{31}$$

$$\begin{aligned}
M_{eK} = & \frac{16}{\sqrt{3}}G_F\pi C_F m_B^4 \int_0^1 dx_1 dx_2 dx_3 \int_0^\infty b_1 db_1 b_3 db_3 \phi_B(x_1, b_1)\phi_{K^*}(\bar{x}_3) \\
& \times \{ [-r_K x_2 (\phi_K^P(\bar{x}_2) + \phi_K^T(\bar{x}_2)) + (1 - x_3)\phi_K^A(\bar{x}_2)] \\
& \cdot E'_e(t_b)h_n(x_1, x_2, 1 - x_3, b_1, b_3) + E'_e(t'_b)h_n(x_1, x_2, x_3, b_1, b_3) \\
& \cdot [-(x_2 + x_3)\phi_K^A(\bar{x}_2) + r_K x_2 (\phi_K^P(\bar{x}_2) - \phi_K^T(\bar{x}_3))] \} , \tag{32}
\end{aligned}$$

$$\begin{aligned}
M_{eK}^{P1} = & -\frac{16}{\sqrt{3}}G_F\pi C_F m_B^4 r_{K^*} \int_0^1 dx_1 dx_2 dx_3 \int_0^\infty b_1 db_1 b_3 db_3 \phi_B(x_1, b_1) \times \{ [(1 - x_3)\phi_K^A(\bar{x}_2) \\
& \cdot (\phi_{K^*}^s(\bar{x}_3) - \phi_{K^*}^t(\bar{x}_3)) + r_K(1 - x_3) (\phi_K^P(\bar{x}_2) + \phi_K^T(\bar{x}_2)) (\phi_{K^*}^s(\bar{x}_3) - \phi_{K^*}^t(\bar{x}_3)) \\
& + r_K x_2 (\phi_K^P(\bar{x}_2) - \phi_K^T(\bar{x}_2)) (\phi_{K^*}^s(\bar{x}_3) + \phi_{K^*}^t(\bar{x}_3))] E'_e(t_b)h_n(x_1, x_2, 1 - x_3, b_1, b_3) \\
& - [x_3 \cdot \phi_K^A(\bar{x}_2) (\phi_{K^*}^s(\bar{x}_3) + \phi_{K^*}^t(\bar{x}_3)) + r_K x_3 (\phi_K^P(\bar{x}_2) + \phi_K^T(\bar{x}_2)) (\phi_{K^*}^s(\bar{x}_3) \\
& + \phi_{K^*}^t(\bar{x}_3)) + r_K x_2 (\phi_K^P(\bar{x}_2) - \phi_K^T(\bar{x}_2)) (\phi_{K^*}^s(\bar{x}_3) - \phi_{K^*}^t(\bar{x}_3))] \\
& \times E'_e(t'_b)h_n(x_1, x_2, x_3, b_1, b_3) \} . \tag{33}
\end{aligned}$$

$$\begin{aligned}
M_{aK} &= \frac{16}{\sqrt{3}} G_F \pi C_F m_B^4 \int_0^1 dx_1 dx_2 dx_3 \int_0^\infty b_1 db_1 b_3 db_3 \phi_B(x_1, b_1) \\
&\times \left\{ [(1-x_2)\phi_K^A(\bar{x}_2)\phi_{K^*}(\bar{x}_3) - r_K r_{K^*}(1-x_2)(\phi_K^P(\bar{x}_2) + \phi_K^T(\bar{x}_2))(\phi_{K^*}^s(\bar{x}_3) - \phi_{K^*}^t(\bar{x}_3)) - r_K r_{K^*} x_3(\phi_K^P(\bar{x}_2) - \phi_K^T(\bar{x}_2))(\phi_{K^*}^s(\bar{x}_3) + \phi_{K^*}^t(\bar{x}_3))] \right. \\
&\times E'_a(t_c) h_{na}(x_1, x_2, x_3, b_1, b_3) - E'_a(t'_c) h'_{na}(x_1, x_2, x_3, b_1, b_3) [x_3 \phi_K^A(\bar{x}_2) \phi_{K^*}(\bar{x}_3) \\
&- 4r_K r_{K^*} \phi_K^P(\bar{x}_2) \phi_{K^*}^s(\bar{x}_3) - r_K r_{K^*}(1-x_3)(\phi_K^P(\bar{x}_2) + \phi_K^T(\bar{x}_2))(\phi_{K^*}^s(\bar{x}_3) \\
&- \phi_{K^*}^t(\bar{x}_3)) + r_K r_{K^*} x_2(\phi_K^P(\bar{x}_2) - \phi_K^T(\bar{x}_2))(\phi_{K^*}^s(\bar{x}_3) + \phi_{K^*}^t(\bar{x}_3))] \left. \right\}, \quad (34)
\end{aligned}$$

$$\begin{aligned}
M_{aK}^{P1} &= \frac{16}{\sqrt{3}} G_F \pi C_F m_B^4 \int_0^1 dx_1 dx_2 dx_3 \int_0^\infty b_1 db_1 b_3 db_3 \phi_B(x_1, b_1) \\
&\left\{ [(1-x_2)r_{K^*} \phi_{K^*}(\bar{x}_3)(\phi_K^P(\bar{x}_2) + \phi_K^T(\bar{x}_2)) - r_{K^*} x_3 \phi_K^A(\bar{x}_2)(\phi_{K^*}^s(\bar{x}_3) - \phi_{K^*}^t(\bar{x}_3))] \right. \\
&\times E'_a(t_c) h_{na}(x_1, x_2, x_3, b_1, b_3) - [(x_2+1)r_K \phi_{K^*}(\bar{x}_3)(\phi_K^P(\bar{x}_2) + \phi_K^T(\bar{x}_2)) \\
&- r_{K^*}(x_3-2)\phi_K^A(\bar{x}_2)(\phi_{K^*}^s(\bar{x}_3) - \phi_{K^*}^t(\bar{x}_3))] E'_a(t'_c) h'_{na}(x_1, x_2, x_3, b_1, b_3) \left. \right\}, \quad (35)
\end{aligned}$$

$$\begin{aligned}
M_{aK}^{P2} &= \frac{16}{\sqrt{3}} G_F \pi C_F m_B^4 \int_0^1 dx_1 dx_2 dx_3 \int_0^\infty b_1 db_1 b_3 db_3 \phi_B(x_1, b_1) \{ [(x_2-1) \\
&\times \phi_K^A(\bar{x}_2) \phi_{K^*}(\bar{x}_3) + 4r_{K^*} r_K \phi_K^P(\bar{x}_2) \phi_{K^*}^s(\bar{x}_3) - r_{K^*} r_K x_2(\phi_K^P(\bar{x}_2) + \phi_K^T(\bar{x}_2)) \\
&\cdot (\phi_{K^*}^s(\bar{x}_3) - \phi_{K^*}^t(\bar{x}_3)) - r_K r_{K^*}(1-x_3)(\phi_K^P(\bar{x}_2) - \phi_K^T(\bar{x}_2))(\phi_{K^*}^s(\bar{x}_3) + \phi_{K^*}^t(\bar{x}_3))] \\
&\cdot E'_a(t_e) h_{na}(x_1, x_2, x_3, b_1, b_3) + [x_3 \phi_K^A(\bar{x}_2) \phi_{K^*}(\bar{x}_3) - x_3 r_K r_{K^*}(\phi_K^P(\bar{x}_2) + \phi_K^T(\bar{x}_2)) \\
&\cdot (\phi_{K^*}^s(\bar{x}_3) - \phi_{K^*}^t(\bar{x}_3)) - r_K r_{K^*}(1-x_2)(\phi_K^P(\bar{x}_2) - \phi_K^T(\bar{x}_2))(\phi_{K^*}^s(\bar{x}_3) + \phi_{K^*}^t(\bar{x}_3))] \\
&\times E'_a(t'_e) h'_{na}(x_1, x_2, x_3, b_1, b_3) \left. \right\}. \quad (36)
\end{aligned}$$

$$\begin{aligned}
F_{aK} &= F_{aK}^{P1} = 4\sqrt{2} G_F \pi C_F f_B m_B^4 \int_0^1 dx_2 dx_3 \int_0^\infty b_2 db_2 b_3 db_3 \left\{ -[(1-x_2)\phi_K^A(\bar{x}_2) \right. \\
&\cdot \phi_{K^*}(\bar{x}_3) - 4r_{K^*} r_K \phi_K^P(\bar{x}_2) \phi_{K^*}^s(\bar{x}_3) + 2r_K r_{K^*} x_2 \phi_{K^*}^s(\bar{x}_3)(\phi_K^P(\bar{x}_2) + \phi_K^T(\bar{x}_2))] \\
&\cdot E_a(t_d) h_a(x_3, 1-x_2, b_3, b_2) + [x_3 \phi_K^A(\bar{x}_2) \phi_{K^*}(\bar{x}_3) - 2r_{K^*} r_K \phi_K^P(\bar{x}_2) \\
&\cdot (\phi_{K^*}^s(\bar{x}_3) + \phi_{K^*}^t(\bar{x}_3)) - 2r_{K^*} r_K x_3 \phi_K^P(\bar{x}_2)(\phi_{K^*}^s(\bar{x}_3) - \phi_{K^*}^t(\bar{x}_3))] \\
&\times E_a(t'_d) h_a(1-x_2, x_3, b_2, b_3) \left. \right\}, \quad (37)
\end{aligned}$$

$$\begin{aligned}
F_{aK}^{P2} &= 8\sqrt{2} G_F \pi C_F f_B m_B^4 \int_0^1 dx_2 dx_3 \int_0^\infty b_2 db_2 b_3 db_3 \\
&\times \left\{ [r_K(1-x_2)(\phi_K^P(\bar{x}_2) - \phi_K^T(\bar{x}_2))\phi_{K^*}(\bar{x}_3) - 2r_{K^*} \phi_K^A(\bar{x}_2) \phi_{K^*}^s(\bar{x}_3)] \right. \\
&\times E_a(t_d) h_a(x_3, 1-x_2, b_3, b_2) \\
&+ [2r_K \phi_K^P(\bar{x}_2) \phi_{K^*}(\bar{x}_3) - x_3 r_{K^*} \phi_K^A(\bar{x}_2)(\phi_{K^*}^s(\bar{x}_3) + \phi_{K^*}^t(\bar{x}_3))] \\
&\times E_a(t'_d) h_a(1-x_2, x_3, b_2, b_3) \left. \right\}. \quad (38)
\end{aligned}$$

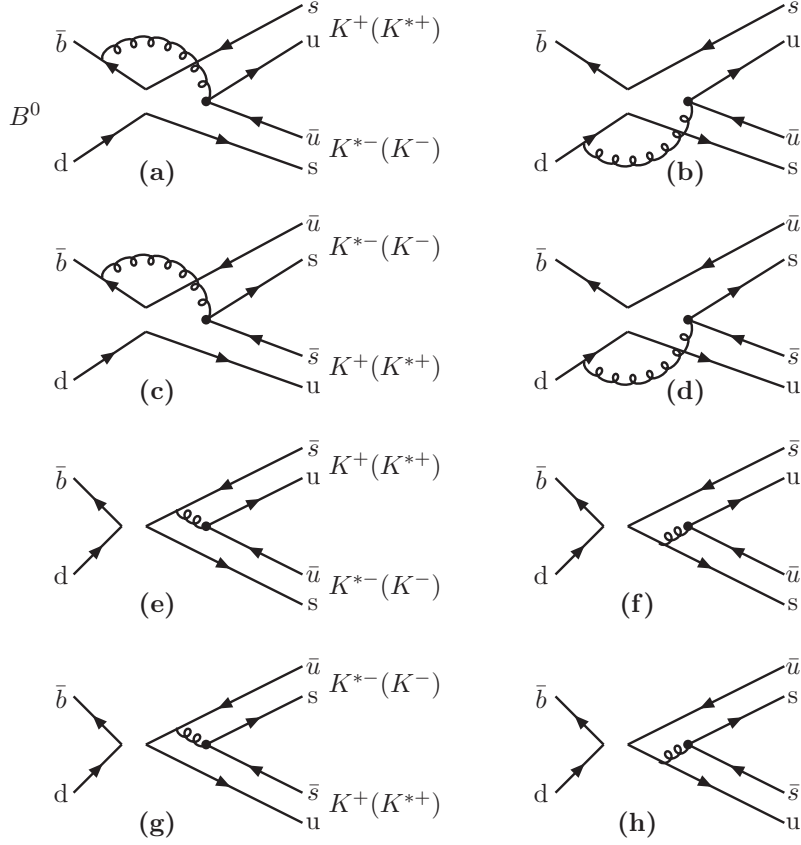


FIG. 2: Diagrams contributing to the $B \rightarrow K^+ K^{*-} (K^{*+} K^-)$ decays.

Combining the contributions from different diagrams in Fig. 1, the total decay amplitude for $B^0 \rightarrow K^{*0} \bar{K}^0$ and $K^0 \bar{K}^{*0}$ decay can be written as

$$\begin{aligned}
\mathcal{M}(B^0 \rightarrow K^{*0} \bar{K}^0 + K^0 \bar{K}^{*0}) = & -\xi_t \left\{ (F_{eK} + F_{eK}^*) \left(a_4 - \frac{1}{2} a_{10} \right) + F_{eK}^{P_2} \left(a_6 - \frac{1}{2} a_8 \right) \right. \\
& + (M_{eK} + M_{eK}^*) \left(C_3 - \frac{1}{2} C_9 \right) + (M_{eK}^{P_1} + M_{eK}^{P_1*}) \left(C_5 - \frac{1}{2} C_7 \right) \\
& + (M_{aK} + M_{aK^*}) \left(C_3 + 2C_4 - \frac{1}{2} C_9 - C_{10} \right) \\
& + (M_{aK}^{P_1} + M_{aK}^{P_1*}) \left(C_5 - \frac{1}{2} C_7 \right) + (M_{aK}^{P_2} + M_{aK}^{P_2*}) (2C_6 - C_8) \\
& + F_{aK} \left(2a_3 + a_4 + 2a_5 - a_7 - a_9 - \frac{1}{2} a_{10} \right) \\
& \left. + F_{aK^*} \left(2a_3 + a_4 - a_9 - \frac{1}{2} a_{10} \right) + (F_{aK}^{P_2} + F_{aK}^{P_2*}) \left(a_6 - \frac{1}{2} a_8 \right) \right\} \quad (39)
\end{aligned}$$

For $B^0 \rightarrow K^+ K^{*-} (K^{*+} K^-)$ decays as illustrated in Fig.2, only annihilation diagrams contribute at leading order. Again, both B^0 and \bar{B}^0 mesons can decay into the final state $K^+ K^{*-}$ and its charge-conjugate state $K^- K^{*+}$. For $B^+ \rightarrow K^+ \bar{K}^{*0}$ and $K^{*+} \bar{K}^0$ decays,

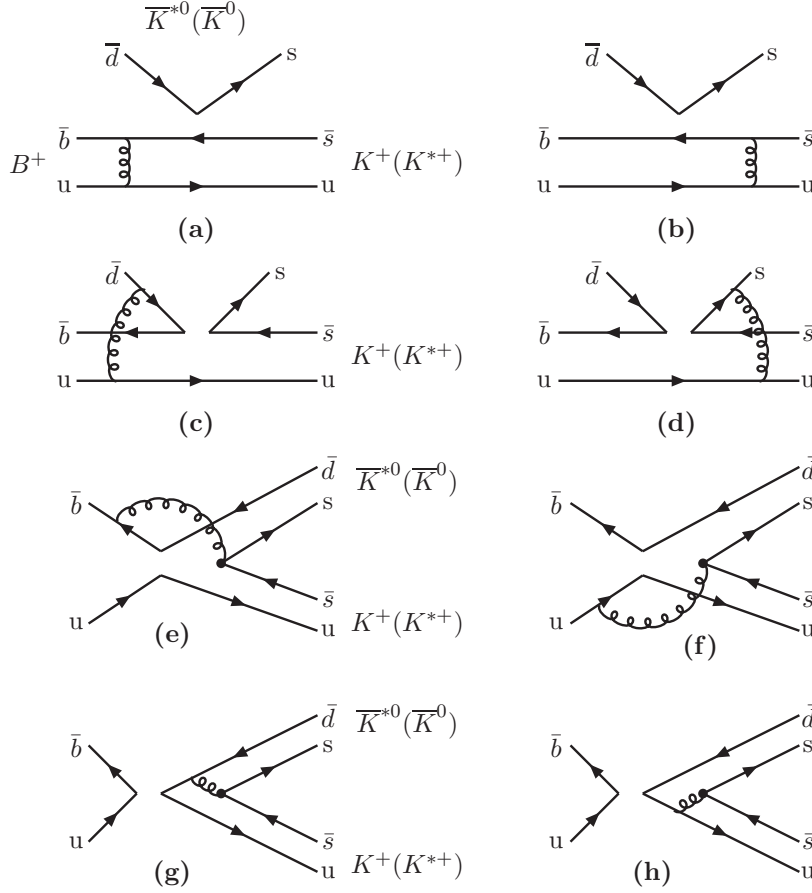


FIG. 3: Diagrams contributing to the $B^+ \rightarrow K^+ \bar{K}^{*0} (K^{*+} \bar{K}^0)$ decays.

as shown in Fig. 3, the factorizable emission diagram, the non-factorizable spectator and annihilation diagrams contribute simultaneously.

Following the same procedure as for $B^0 \rightarrow K^{*0} \bar{K}^0 / K^0 \bar{K}^{*0}$ decays, we find the total decay amplitude for the later two decay modes:

$$\begin{aligned}
\mathcal{M}(B^0 \rightarrow K^+ K^{*-} + K^- K^{*+}) &= \xi_u [(M_{aK} + M_{aK^*}) C_2 + (F_{aK} + F_{aK^*}) a_2] \\
&\quad - \xi_t \left\{ (M_{aK} + M_{aK^*}) \left(2C_4 + \frac{1}{2}C_{10} \right) + (M_{aK}^{P_2} + M_{aK^*}^{P_2}) \left(2C_6 + \frac{1}{2}C_8 \right) \right. \\
&\quad \left. + (F_{aK} + F_{aK^*}) \left(2a_3 + 2a_5 + \frac{1}{2}a_7 + \frac{1}{2}a_9 \right) \right\}. \tag{40}
\end{aligned}$$

$$\begin{aligned}
\mathcal{M}(B^+ \rightarrow K^+ \bar{K}^{*0}) &= \xi_u (M_{aK} C_1 + F_{aK} a_1) - \xi_t \left\{ F_{eK} \left(a_4 - \frac{1}{2}a_{10} \right) \right. \\
&\quad \left. + M_{eK} \left(C_3 - \frac{1}{2}C_9 \right) + M_{eK}^{P_1} \left(C_5 - \frac{1}{2}C_7 \right) + M_{aK} (C_3 + C_9) \right. \\
&\quad \left. + M_{aK}^{P_1} (C_5 + C_7) + F_{aK} (a_4 + a_{10}) + F_{aK}^{P_2} (a_6 + a_8) \right\}, \tag{41}
\end{aligned}$$

$$\begin{aligned}
\mathcal{M}(B^+ \rightarrow K^{*+} \overline{K}^0) &= \xi_u (M_{aK^*} C_1 + F_{aK^*} a_1) \\
&\quad - \xi_t \left\{ F_{eK^*} \left(a_4 - \frac{1}{2} a_{10} \right) + F_{eK^*}^{P_2} \left(a_6 - \frac{1}{2} a_8 \right) \right. \\
&\quad + M_{eK^*} \left(C_3 - \frac{1}{2} C_9 \right) + M_{eK^*}^{P_1} \left(C_5 - \frac{1}{2} C_7 \right) \\
&\quad + M_{aK^*} (C_3 + C_9) + M_{aK^*}^{P_1} (C_5 + C_7) \\
&\quad \left. + F_{aK^*} (a_4 + a_{10}) + F_{aK^*}^{P_2} (a_6 + a_8) \right\}, \tag{42}
\end{aligned}$$

In the decay amplitudes of Eqs.(39) - (42), the coefficients a_i , the standard combination of the Wilson coefficients C_i , have been defined as usual

$$\begin{aligned}
a_1 &= C_2 + \frac{C_1}{3}, \quad a_2 = C_1 + \frac{C_2}{3}, \\
a_i &= C_i + \frac{C_{i+1}}{3}, \quad \text{for } i = 3, 5, 7, 9, \\
a_i &= C_i + \frac{C_{i-1}}{3}, \quad \text{for } i = 4, 6, 8, 10. \tag{43}
\end{aligned}$$

Based on these decay amplitudes, the leading order pQCD predictions for the branching ratios and CP violating asymmetries of the considered decays can be calculated [10].

IV. NLO CONTRIBUTIONS TO $B \rightarrow KK^*$ DECAYS IN PQCD

The power counting in the pQCD factorization approach [13] is different from that in the QCD factorization[3]. When compared with the previous LO calculations in pQCD [10], the following NLO contributions will be included:

1. The LO Wilson coefficients $C_i(m_W)$ will be replaced by those at NLO level in NDR scheme [16]. As mentioned in last section, the strong coupling constant $\alpha_s(t)$ at two-loop level as given in Eq. (8), and the NLO RG evolution matrix $U(t, m, \alpha)$, as defined in Ref. [16], will be used here:

$$U(m_1, m_2, \alpha) = U(m_1, m_2) + \frac{\alpha}{4\pi} R(m_1, m_2) \tag{44}$$

where the function $U(m_1, m_2)$ and $R(m_1, m_2)$ represent the QCD and QED evolution and have been defined in Eq. (6.24) and (7.22) in Ref. [16]. We also introduce a cut-off $\Lambda_{cut} = 1$ GeV for low energy scale in the final integration.

2. The NLO contributions to the hard kernel H , including the vertex corrections, the quark loops, and the magnetic penguin [13].

A. Vertex corrections

The vertex corrections to the factorizable emission diagrams, as illustrated by Fig. (2), have been calculated years ago in the QCD factorization approach[3, 20]. According to

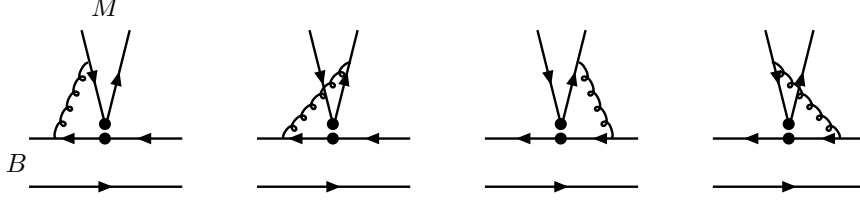


FIG. 4: NLO vertex corrections to the factorizable amplitudes.

Ref. [13], the difference of the calculations induced by considering or not considering the parton transverse momentum is rather small, say less than 10%, and therefore can be neglected. Consequently, one can use the vertex corrections as given in Ref. [20] directly. The vertex corrections can be absorbed into the re-definition of the Wilson coefficients $a_i(\mu)$ by adding a vertex-function $V_i(M)$ to them [3, 20]

$$\begin{aligned}
 a_i(\mu) &\rightarrow a_i(\mu) + \frac{\alpha_s(\mu)}{4\pi} C_F \frac{C_i(\mu)}{3} V_i(M), \quad \text{for } i = 1, 2; \\
 a_j(\mu) &\rightarrow a_j(\mu) + \frac{\alpha_s(\mu)}{4\pi} C_F \frac{C_{j\pm 1}(\mu)}{N_c} V_j(M), \quad \text{for } j = 3 - 10,
 \end{aligned} \tag{45}$$

where M is the meson emitted from the weak vertex. When M is a pseudo-scalar meson, the vertex functions $V_i(M)$ are given (in the NDR scheme) in Refs. [13, 20]:

$$V_i(M) = \begin{cases} 12 \ln \frac{m_b}{\mu} - 18 + \frac{2\sqrt{2N_c}}{f_M} \int_0^1 dx \phi_M^A(x) g(x), & \text{for } i = 1 - 4, 9, 10, \\ -12 \ln \frac{m_b}{\mu} + 6 - \frac{2\sqrt{2N_c}}{f_M} \int_0^1 dx \phi_M^A(x) g(1-x), & \text{for } i = 5, 7, \\ -6 + \frac{2\sqrt{2N_c}}{f_M} \int_0^1 dx \phi_M^P(x) h(x), & \text{for } i = 6, 8, \end{cases} \tag{46}$$

where f_M is the decay constant of the meson M ; $\phi_M^A(x)$ and $\phi_M^P(x)$ are the twist-2 and twist-3 distribution amplitude of the meson M , respectively. For a vector meson M , $\phi_M^A(\phi_M^P)$ is replaced by $\phi_M(\phi_M^s)$ and f_M by f_M^T in the third line of the above formulas. The hard-scattering functions $g(x)$ and $h(x)$ in Eq. (46) are:

$$\begin{aligned}
 g(x) &= 3 \left(\frac{1-2x}{1-x} \ln x - i\pi \right) \\
 &\quad + \left[2Li_2(x) - \ln^2 x + \frac{2 \ln x}{1-x} - (3 + 2i\pi) \ln x - (x \leftrightarrow 1-x) \right], \tag{47}
 \end{aligned}$$

$$h(x) = 2Li_2(x) - \ln^2 x - (1 + 2i\pi) \ln x - (x \leftrightarrow 1-x), \tag{48}$$

where $Li_2(x)$ is the dilogarithm function. As shown in Ref. [13], the μ -dependence of the Wilson coefficients $a_i(\mu)$ will be improved generally by the inclusion of the vertex corrections.

B. Quark loops

The contribution from the so-called ‘‘quark-loops’’ is a kind of penguin correction with the four quark operators insertion, as illustrated by Fig. (5). In fact this is generally

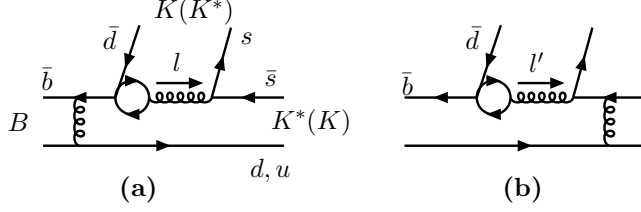


FIG. 5: Quark-loop diagrams contributing to $B^0 \rightarrow K^{*0}\bar{K}^0 + K^0\bar{K}^{*0}$, $B^+ \rightarrow K^{*+}\bar{K}^0$ and $K^+\bar{K}^{*0}$ decays.

called BSS mechanism[21], which plays a very important role in CP violation. We here include quark-loop amplitude from the operators $O_{1,2}$ and O_{3-6} only. The quark loops from O_{7-10} will be neglected due to their smallness.

For the $b \rightarrow d$ transition, the contributions from the various quark loops are described by the effective Hamiltonian $H_{eff}^{(q)}$ [13],

$$H_{eff}^{(q)} = - \sum_{q=u,c,t} \sum_{q'} \frac{G_F}{\sqrt{2}} V_{qb} V_{qd}^* \frac{\alpha_s(\mu)}{2\pi} C^{(q)}(\mu, l^2) (\bar{d}\gamma_\rho (1 - \gamma_5) T^{ab}) (\bar{q}'\gamma^\rho T^a q'), \quad (49)$$

where l^2 being the invariant mass of the gluon, which connects the quark loops with the $\bar{q}'q$ pair as shown in Fig. 5. The functions $C^{(q)}(\mu, l^2)$ can be written as

$$C^{(q)}(\mu, l^2) = \left[G^{(q)}(\mu, l^2) - \frac{2}{3} \right] C_2(\mu), \quad (50)$$

for $q = u, c$ and

$$C^{(t)}(\mu, l^2) = \left[G^{(s)}(\mu, l^2) - \frac{2}{3} \right] C_3(\mu) + \sum_{q''=u,d,s,c} G^{(q'')}(\mu, l^2) [C_4(\mu) + C_6(\mu)]. \quad (51)$$

The integration function $G^{(q)}(\mu, l^2)$ for the loop of the quarks $q = (u, d, s, c)$ is defined as [13]

$$G^{(q)}(\mu, l^2) = -4 \int_0^1 dx x(1-x) \ln \frac{m_q^2 - x(1-x)l^2}{\mu^2}, \quad (52)$$

where m_q is the quark mass. The explicit expressions of the function $G^{(q)}(\mu, l^2)$ after the integration can be found, for example, in Ref. [13].

It is straightforward to calculate the decay amplitude for Fig.(5)a and (5)b. For the case of $B \rightarrow K^*$ or $B \rightarrow K$ transition, we find the corresponding decay amplitude $M_{K^*K}^{(q)}$

and $M_{KK^*}^{(q)}$ with $q = u, c, t$, respectively;

$$\begin{aligned}
M_{K^*K}^{(q)} &= -\frac{4}{\sqrt{3}}G_F C_F^2 m_B^4 \int_0^1 dx_1 dx_2 dx_3 \int_0^\infty b_1 db_1 b_2 db_2 \phi_B(x_1, b_1) \\
&\cdot \left\{ \left\{ (1+x_2) \phi_{K^*}(\bar{x}_2) \phi_K^A(\bar{x}_3) \right. \right. \\
&\quad - r_{K^*} (1-2x_2) \left[\phi_{K^*}^s(\bar{x}_2) - \phi_{K^*}^t(\bar{x}_2) \right] \phi_K^A(\bar{x}_3) - 2r_K \phi_{K^*}(\bar{x}_2) \phi_K^P(\bar{x}_3) \\
&\quad \left. \left. + 2r_{K^*} r_K \left[(2+x_2) \phi_{K^*}^s(\bar{x}_2) + x_2 \phi_{K^*}^t(\bar{x}_2) \right] \phi_K^P(\bar{x}_3) \right\} \right. \\
&\quad \cdot E^{(q)}(t_q, l^2) h_e(x_2, x_1, b_2, b_1) \\
&\quad \left. + \left\{ -2r_{K^*} \phi_{K^*}^s(\bar{x}_2) \phi_K^A(\bar{x}_3) + 4r_{K^*} r_K \phi_{K^*}^s(\bar{x}_2) \phi_K^P(\bar{x}_3) \right\} \right. \\
&\quad \left. \cdot E^{(q)}(t'_q, l^2) h_e(x_1, x_2, b_1, b_2) \right\} \tag{53}
\end{aligned}$$

and

$$\begin{aligned}
M_{KK^*}^{(q)} &= -\frac{4}{\sqrt{3}}G_F C_F^2 m_B^4 \int_0^1 dx_1 dx_2 dx_3 \int_0^\infty b_1 db_1 b_2 db_2 \phi_B(x_1, b_1) \\
&\cdot \left\{ \left\{ (1+x_2) \phi_K^A(\bar{x}_2) \phi_{K^*}(\bar{x}_3) \right. \right. \\
&\quad + r_K (1-2x_2) \left[\phi_K^P(\bar{x}_2) - \phi_K^T(\bar{x}_2) \right] \phi_{K^*}(\bar{x}_3) - 2r_{K^*} \phi_K^A(\bar{x}_2) \phi_{K^*}^s(\bar{x}_3) \\
&\quad \left. \left. - 2r_K r_{K^*} \left[(2+x_2) \phi_K^P(\bar{x}_2) + x_2 \phi_K^T(\bar{x}_2) \right] \phi_{K^*}^s(\bar{x}_3) \right\} \right. \\
&\quad \cdot E^{(q)}(t_q, l^2) h_e(x_2, x_1, b_2, b_1) \\
&\quad \left. + \left\{ 2r_K \phi_K^P(\bar{x}_2) \phi_{K^*}(\bar{x}_3) - 4r_K r_{K^*} \phi_K^P(\bar{x}_2) \phi_{K^*}^s(\bar{x}_3) \right\} \right. \\
&\quad \left. \cdot E^{(q)}(t'_q, l^2) h_e(x_1, x_2, b_1, b_2) \right\}, \tag{54}
\end{aligned}$$

where $r_K = m_0^K/m_B$, $r_{K^*} = m_{K^*}/m_B$, the evolution factors take the form of

$$E^{(q)}(t, l^2) = C^{(q)}(t, l^2) \alpha_s^2(t) \cdot \exp[-S_{ab}], \tag{55}$$

with the Sudakov factor S_{ab} and the hard function $h_e(x_1, x_2, b_1, b_2)$ as given in Eq. (A9) and Eq. (A1) respectively, and finally the hard scales and the gluon invariant masses are

$$\begin{aligned}
t_q &= \max(\sqrt{x_2}m_B, \sqrt{x_1 x_2}m_B, \sqrt{(1-x_2)x_3}m_B, 1/b_1, 1/b_2);, \\
t'_q &= \max(\sqrt{x_1}m_B, \sqrt{x_1 x_2}m_B, \sqrt{|x_3 - x_1|}m_B, 1/b_1, 1/b_2), \tag{56}
\end{aligned}$$

$$\begin{aligned}
l^2 &= (1-x_2)x_3 m_B^2 - |\mathbf{k}_{2T} - \mathbf{k}_{3T}|^2 \approx (1-x_2)x_3 m_B^2, \\
l'^2 &= (x_3 - x_1)m_B^2 - |\mathbf{k}_{1T} - \mathbf{k}_{3T}|^2 \approx (x_3 - x_1)m_B^2. \tag{57}
\end{aligned}$$

Finally, the total ‘‘quark-loop’’ contribution to the considered $B \rightarrow KK^*$ decays can be written as

$$M_{KK^*}^{(q)} = \langle K^* K | \mathcal{H}_{eff}^q | B \rangle = \sum_{q=u,c,t} \lambda_q \left[M_{K^*K}^{(q)} + M_{KK^*}^{(q)} \right], \tag{58}$$

where $\lambda_q = V_{qb}V_{qd}^*$.

From the functions $C^{(q)}(\mu, l^2)$, one can see that the quark-loop amplitudes depend on both the renormalization scale μ and the gluon invariant mass l^2 . In the naive factorization approach, the assumption of a constant l^2 , $l^2 \sim m_b^2/2$, introduces a large theoretical

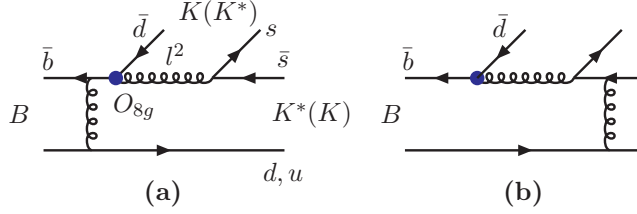


FIG. 6: Chromo-magnetic penguin (O_{8g}) diagrams contributing to $B^0 \rightarrow K^{*0}\bar{K}^0 + K^0\bar{K}^{*0}$, $B^+ \rightarrow K^{*+}\bar{K}^0$ and $K^+\bar{K}^{*0}$ decays.

uncertainty as making predictions. In the pQCD approach, however, l^2 is related to the parton momenta unambiguously. Because of the absence of the end-point singularities associated with $l^2, l' \rightarrow 0$, in Fig. (5)a and (5)b respectively, we have dropped the parton transverse momenta k_T in l^2, l'^2 for simplicity [13].

From Fig. (5), it is easy to see that the "quark-loop" diagrams contribute only to $B^0 \rightarrow K^{*0}\bar{K}^0 + K^0\bar{K}^{*0}$ and $B^+ \rightarrow K^{*+}\bar{K}^0, K^+\bar{K}^{*0}$ decays. For $B^0 \rightarrow K^+K^{*-}$ and $K^{*+}K^-$ decays, there is no such kind of NLO contributions.

C. Chromo-magnetic penguin contributions

As illustrated by Fig. (6), the chromo-magnetic penguin operator O_{8g} also contribute to $B \rightarrow KK^*$ decays at NLO level. The corresponding weak effective Hamiltonian contains the $b \rightarrow dg$ transition,

$$\mathcal{H}_{eff}^{cmp} = -\frac{G_F}{\sqrt{2}}V_{tb}V_{td}^* C_{8g}^{eff} O_{8g}, \quad (59)$$

with the chromo-magnetic penguin operator,

$$O_{8g} = \frac{g_s}{8\pi^2}m_b \bar{d}_i\sigma^{\mu\nu}(1 + \gamma_5)T_{ij}^a G_{\mu\nu}^a b_j, \quad (60)$$

where i, j being the color indices of quarks. The corresponding effective Wilson coefficient $C_{8g}^{eff} = C_{8g} + C_5$ [13].

In Ref. [22], the authors calculated the chromo-magnetic penguin contributions to $B \rightarrow \phi K$ decays using the pQCD approach. They considered nine chromo-magnetic penguin diagrams corresponding to the non-local operator O'_{8g} , as given in Eq. (2.3) of Ref. [22], generated by operator O_{8g} as defined in Eq. (60). The first two Feynman diagrams (a) and (b) in Ref. [22] are the same as Figs. (6)a and (6)b here. According to Ref. [22], the diagrams (a) and (b) dominate, while other seven diagrams are small or negligible. It is therefore reasonable for us to consider the NLO contributions induced by the diagrams (a) and (b) only, for the sake of simplicity.

The decay amplitude for Figs. 6a and 6b can be written as

$$\begin{aligned}
M_{K^*K}^{(g)} = & \frac{4}{\sqrt{3}} G_F C_F^2 m_B^6 \int_0^1 dx_1 dx_2 dx_3 \int_0^\infty b_1 db_1 b_2 db_2 \phi_B(x_1, b_1) \\
& \cdot \left\{ \left\{ -(1-x_2) \left[2\phi_{K^*}(\bar{x}_2) - r_{K^*} \left[3\phi_{K^*}^s(\bar{x}_2) - \phi_{K^*}^t(\bar{x}_2) \right] \right. \right. \right. \\
& \left. \left. \left. - r_{K^*} x_2 \left[\phi_{K^*}^s(\bar{x}_2) + \phi_{K^*}^t(\bar{x}_2) \right] \right] \phi_{K^*}^A(\bar{x}_3) \right. \right. \\
& \left. \left. + r_K (1+x_2) x_3 \cdot \phi_{K^*}(\bar{x}_2) \left[3\phi_{K^*}^P(\bar{x}_3) + \phi_{K^*}^T(\bar{x}_3) \right] \right. \right. \\
& \left. \left. - r_{K^*} r_K (1-x_2) \left[\phi_{K^*}^s(\bar{x}_2) + \phi_{K^*}^t(\bar{x}_2) \right] \left[3\phi_{K^*}^P(\bar{x}_3) - \phi_{K^*}^T(\bar{x}_3) \right] \right. \right. \\
& \left. \left. - r_{K^*} r_K x_3 (1-2x_2) \left[\phi_{K^*}^s(\bar{x}_2) - \phi_{K^*}^t(\bar{x}_2) \right] \left[3\phi_{K^*}^P(\bar{x}_3) + \phi_{K^*}^T(\bar{x}_3) \right] \right\} \right. \\
& \cdot E_g(t_q) h_g(A, B, C, b_1, b_2, b_3, x_2) \\
& \left. + \left\{ 4r_{K^*} \phi_{K^*}^s(\bar{x}_2) \phi_{K^*}^A(\bar{x}_3) - 2r_{K^*} r_K x_3 \phi_{K^*}^s(\bar{x}_2) \left[3\phi_{K^*}^P(\bar{x}_3) + \phi_{K^*}^T(\bar{x}_3) \right] \right\} \right. \\
& \left. \cdot E_g(t'_q) h_g(A', B', C', b_2, b_1, b_3, x_1) \right\}, \tag{61}
\end{aligned}$$

for the case of $B \rightarrow K^*$ transition, and

$$\begin{aligned}
M_{KK^*}^{(g)} = & \frac{4}{\sqrt{3}} G_F C_F^2 m_B^6 \int_0^1 dx_1 dx_2 dx_3 \int_0^\infty b_1 db_1 b_2 db_2 \phi_B(x_1, b_1) \\
& \left\{ \left\{ -(1-x_2) \left[2\phi_K^A(\bar{x}_2) + r_K \left[3\phi_K^P(\bar{x}_2) - \phi_K^T(\bar{x}_2) \right] \right. \right. \right. \\
& \left. \left. \left. + r_K x_2 \left[\phi_K^P(\bar{x}_2) + \phi_K^T(\bar{x}_2) \right] \right] \phi_{K^*}(\bar{x}_3) \right. \right. \\
& \left. \left. + r_{K^*} (1+x_2) x_3 \phi_K^A(\bar{x}_2) \left[3\phi_{K^*}^s(\bar{x}_3) + \phi_{K^*}^t(\bar{x}_3) \right] \right. \right. \\
& \left. \left. + r_K r_{K^*} (1-x_2) \left[\phi_K^P(\bar{x}_2) + \phi_K^T(\bar{x}_2) \right] \left[3\phi_{K^*}^s(\bar{x}_3) - \phi_{K^*}^t(\bar{x}_3) \right] \right. \right. \\
& \left. \left. + r_K r_{K^*} x_3 (1-2x_2) \left[\phi_K^P(\bar{x}_2) - \phi_K^T(\bar{x}_2) \right] \left[3\phi_{K^*}^s(\bar{x}_3) + \phi_{K^*}^t(\bar{x}_3) \right] \right\} \right. \\
& \cdot E_g(t_q) h_g(A, B, C, b_1, b_2, b_3, x_2) \\
& \left. - \left\{ 4r_K \phi_K^P(\bar{x}_2) \phi_{K^*}(\bar{x}_3) - 2r_K r_{K^*} x_3 \phi_K^P(\bar{x}_2) \left[3\phi_{K^*}^s(\bar{x}_3) + \phi_{K^*}^t(\bar{x}_3) \right] \right\} \right. \\
& \left. \cdot E_g(t'_q) h_g(A', B', C', b_2, b_1, b_3, x_1) \right\}, \tag{62}
\end{aligned}$$

for the case of $B \rightarrow K$ transition. Here the hard scale t_q and t'_q are the same as in Eq. (56). The evolution factor $E_g(t)$ in Eqs. (61) and (62) is of the form

$$E_g(t) = C_{8g}^{eff}(t) \alpha_s^2(t) \cdot \exp[-S_g], \tag{63}$$

with the Sudakov factor S_g and the hard function h_g ,

$$\begin{aligned}
S_{mg}(t) = & s \left(x_1 m_B / \sqrt{2}, b_1 \right) + s \left(x_2 m_B / \sqrt{2}, b_2 \right) + s \left((1-x_2) m_B / \sqrt{2}, b_2 \right) \\
& + s \left(x_3 m_B / \sqrt{2}, b_3 \right) + s \left((1-x_3) m_B / \sqrt{2}, b_3 \right) \\
& - \frac{1}{\beta_1} \left[\ln \frac{\ln(t/\Lambda)}{-\ln(b_1 \Lambda)} + \ln \frac{\ln(t/\Lambda)}{-\ln(b_2 \Lambda)} + \ln \frac{\ln(t/\Lambda)}{-\ln(b_3 \Lambda)} \right], \tag{64}
\end{aligned}$$

$$\begin{aligned}
h_g(A, B, C, b_1, b_2, b_3, x_i) = & -S_t(x_i) K_0(Bb_1) K_0(Cb_3) \\
& \cdot \int_0^{\pi/2} d\theta \tan \theta \cdot J_0(Ab_1 \tan \theta) J_0(Ab_2 \tan \theta) J_0(Ab_3 \tan \theta), \tag{65}
\end{aligned}$$

where the functions $K_0(x)$ and $J_0(x)$ are the Bessel functions, the form factor $S_t(x_i)$ with $i = 1, 2$ has been given in Eq. (A7), and the invariant masses $A^{(i)}, B^{(i)}$ and $C^{(i)}$ of the virtual quarks and gluons are of the form

$$\begin{aligned} A &= \sqrt{x_2}m_B, & B &= B' = \sqrt{x_1x_2}m_B, & C &= i\sqrt{(1-x_2)x_3}m_B, \\ A' &= \sqrt{x_1}m_B, & C' &= \sqrt{x_1-x_3}m_B. \end{aligned} \quad (66)$$

The total ‘‘chromo-magnetic penguin’’ contribution to the considered $B \rightarrow KK^*$ decays can therefore be written as

$$M_{KK^*}^{(cmp)} = \langle K^*K | \mathcal{H}_{eff}^{cmp} | B \rangle = \lambda_t \left[M_{K^*K}^{(g)} + M_{KK^*}^{(g)} \right], \quad (67)$$

where $\lambda_t = V_{tb}V_{td}^*$.

From Fig. (6), one can see that the chromo-magnetic penguins contribute only to $B^0 \rightarrow K^{*0}\bar{K}^0 + K^0\bar{K}^{*0}$ and $B^+ \rightarrow K^{*+}\bar{K}^0, K^+\bar{K}^{*0}$ decays. For $B^0 \rightarrow K^+K^{*-}$ and $K^{*+}K^-$ decays, there is again no such kind of NLO contributions.

V. NUMERICAL RESULTS AND DISCUSSIONS

A. Input parameters

Besides those specified in the text, the following input parameters will also be used in the numerical calculations:

$$\begin{aligned} m_B &= 5.28\text{GeV}, & m_K &= 0.49\text{GeV}, & m_{K^*} &= 0.892\text{GeV}, & m_b &= 4.8\text{GeV}, \\ m_{0K} &= 1.7\text{GeV}, & m_W &= 80.41\text{GeV}, & m_t &= 168\text{GeV}, & \alpha_{em} &= 1/128, \\ f_B &= 0.21\text{GeV}, & f_{K^*} &= 0.217\text{GeV}, & f_{K^*}^T &= f_K = 0.16\text{GeV}, \\ \tau_{B^0} &= 1.528\text{ps}, & \tau_{B^+} &= 1.643\text{ps}, \end{aligned} \quad (68)$$

For the CKM quark-mixing matrix, we use the Wolfenstein parametrization as given in Ref.[23].

$$\begin{aligned} V_{ud} &= 0.9745, & V_{us} &= \lambda = 0.2200, & |V_{ub}| &= 4.31 \times 10^{-3}, \\ V_{cd} &= -0.224, & V_{cd} &= 0.996, & V_{cb} &= 0.0413, \\ |V_{td}| &= 7.4 \times 10^{-3}, & V_{ts} &= -0.042, & |V_{tb}| &= 0.9991, \end{aligned} \quad (69)$$

with the CKM angles $\beta = 21.6^\circ$, $\gamma = 60^\circ \pm 20^\circ$ and $\alpha = 100^\circ \pm 20^\circ$. The unitarity condition $V_{ub}V_{uq}^* + V_{cb}V_{cq}^* + V_{tb}V_{tq}^* = 0$ for $q = d, s$ is employed

B. Branching ratios

In the pQCD approach, the form factor $A_0^{B \rightarrow K^*}(q^2 = 0)$ and $F_{0,1}^{B \rightarrow K}(q^2 = 0)$ can be extracted from the decay amplitude F_{eK^*} and F_{eK} as shown in Eqs. (19) and (30), via

the following relations,

$$F_{0,1}^{B \rightarrow K}(q^2 = 0) = \frac{\sqrt{2} F_{eK}}{G_F f_{K^*} m_B^2}, \quad (70)$$

$$A_0^{B \rightarrow K^*}(q^2 = 0) = \frac{\sqrt{2} F_{eK^*}}{G_F f_K m_B^2}. \quad (71)$$

Consequently, one can find the NLO pQCD predictions for the values of the corresponding form factors at zero momentum transfer:

$$A_0^{B \rightarrow K^*}(q^2 = 0) = 0.38 \pm 0.05(\omega_b), \quad F_{0,1}^{B \rightarrow K}(q^2 = 0) = 0.36 \pm 0.06(\omega_b), \quad (72)$$

for $\omega_b = 0.40 \pm 0.04 \text{ GeV}$, which agree well with those obtained in QCD sum rule calculations, for example, in Refs. [18, 19].

For a general charmless two-body decays $B \rightarrow f$ with $f = M_2 M_3$, the branching ratio can be written in general as

$$Br(B \rightarrow f) = \tau_B \frac{1}{16\pi m_B} |\mathcal{M}|^2 \quad (73)$$

where τ_B is the lifetime of the B meson, and $\mathcal{M} = \langle KK^* | \mathcal{H}_{eff} | B \rangle$ for the case of $f = K K^*$.

Using the wave functions and the input parameters as specified in previous sections, it is straightforward to calculate the branching ratios for the considered decays. For $B^+ \rightarrow K^+ \bar{K}^{*0}$ and $B^+ \rightarrow K^{*+} \bar{K}^0$ decays, we show in Table II, the CP-averaged branching ratios

$$Br(B \rightarrow f) = \frac{1}{2} [Br(B \rightarrow f) + Br(\bar{B} \rightarrow \bar{f})]. \quad (74)$$

For B^0 decays, it is a little complicate since both B^0 and \bar{B}^0 can decay into the final state f and \bar{f} simultaneously. In Table II, we show the CP-averaged Br's for $B^0 \rightarrow f_1$, $B^0 \rightarrow \bar{f}_1$ and for $B^0 \rightarrow f_1 + \bar{f}_1$ with $f_1 = K^0 \bar{K}^{*0}$, respectively. The third result corresponds to the measured upper limit. For $B^0 \rightarrow f_2, \bar{f}_2$ and $B^0 \rightarrow f_2 + \bar{f}_2$ with $f_2 = K^+ K^{*-}$, we take the same convention.

Except for the LO results, we always use the NLO Wilson coefficients in the calculations. The label +VC, +QL, +MP and NLO denote the pQCD predictions with the inclusion of the vertex corrections only, the quark loops only, the magnetic-penguin only, and all the considered NLO corrections, respectively. For the sake of comparison, we also show currently available experimental results [24] and the numerical results evaluated in the framework of the QCD factorization (QCDF) [20].

It is worth stressing that the theoretical predictions in the pQCD approach have relatively large theoretical errors induced by the still large uncertainties of many input parameters. The pQCD predictions for the branching ratios with the consideration of

TABLE II: The pQCD predictions for the branching ratios (in unit of 10^{-7}). The label LO means the leading-order results, and +VC, +QL, +MP, NLO mean the predictions with the inclusion of the vertex corrections, the quark loops, the magnetic-penguin, and all the considered NLO corrections, respectively.

Mode	LO	+VC	+QL	+MP	NLO	Data	QCDF
$B^+ \rightarrow K^+ \overline{K}^{*0}$	4.2	5.3	5.8	3.1	3.2	< 11	$3.0^{+6.0}_{-2.5}$
$B^+ \rightarrow K^{*+} \overline{K}^0$	2.0	2.7	2.3	1.6	2.1		$3.0^{+7.2}_{-2.7}$
$B^0 \rightarrow K^0 \overline{K}^{*0}$	2.1	3.0	2.9	1.8	2.4	–	$2.6^{+2.8}_{-2.0}$
$B^0 \rightarrow \overline{K}^0 K^{*0}$	6.4	6.9	8.0	4.3	4.9	–	$2.9^{+7.3}_{-2.7}$
$B^0 \rightarrow K^0 \overline{K}^{*0} + K^0 K^{*0}$	13.7	14.0	15.2	6.7	8.5	< 19	
$B^0 \rightarrow K^+ \overline{K}^{*-}$	1.1	–	–	–	0.83		$0.14^{+1.07}_{-0.14}$
$B^0 \rightarrow K^- \overline{K}^{*+}$	0.41	–	–	–	0.17		$0.14^{+1.07}_{-0.14}$
$B^0 \rightarrow K^+ \overline{K}^{*-} + K^- \overline{K}^{*+}$	2.7	–	–	–	1.3		

major uncertainties are the following (in unit of 10^{-7})

$$\begin{aligned}
Br(B^+ \rightarrow K^+ \overline{K}^{*0}) &= 3.2^{+1.0}_{-0.6}(\omega_b)^{+0.2}_{-0.1}(\alpha)^{+0.5}_{-0.3}(a_{iK})^{+0.2}_{-0.1}(a_{iK^*}), \\
Br(B^+ \rightarrow K^{*+} \overline{K}^0) &= 2.1^{+0.1}_{-0.2}(\omega_b)^{+0.2}_{-0.3}(\alpha)^{+1.3}_{-1.2}(a_{iK}) \pm 0.4(a_{iK^*}), \\
Br(B^0 \rightarrow K^0 \overline{K}^{*0}) &= 2.4 \pm 0.2(\omega_b)^{+0.0}_{-0.1}(\alpha)^{+0.3}_{-0.4}(a_{iK})^{+0.6}_{-0.4}(a_{iK^*}), \\
Br(B^0 \rightarrow \overline{K}^0 K^{*0}) &= 4.9^{+1.2}_{-0.8}(\omega_b)^{+0.3}_{-0.2}(\alpha)^{+0.5}_{-0.4}(a_{iK})^{+0.3}_{-0.1}(a_{iK^*}), \\
Br(B^0 \rightarrow f_1 + \bar{f}_1) &= 8.5^{+2.2}_{-1.7}(\omega_b) \pm 0.1(\alpha)^{+1.0}_{-0.9}(a_{iK})^{+1.1}_{-0.6}(a_{iK^*}), \\
Br(B^0 \rightarrow K^+ K^{*-}) &= 0.83^{+0.04}_{-0.08}(\omega_b) \pm 0.6(\alpha)^{+0.28}_{-0.21}(a_{iK})^{+0.28}_{-0.18}(a_{iK^*}), \\
Br(B^0 \rightarrow K^- K^{*+}) &= 0.17^{+0.02}_{-0.01}(\omega_b) \pm 0.07(\alpha)^{+0.26}_{-0.08}(a_{iK}) \pm 0.02(a_{iK^*}), \\
Br(B^0 \rightarrow f_2 + \bar{f}_2) &= 1.3 \pm 0.1(\omega_b)^{+0.0}_{-0.1}(\alpha)^{+0.2}_{-0.6}(a_{iK})^{+0.4}_{-0.3}(a_{iK^*}). \tag{75}
\end{aligned}$$

The major theoretical errors are induced by the uncertainties of $\omega_b = 0.4 \pm 0.04$ GeV, $\alpha = 100^\circ \pm 20^\circ$, and Gegenbauer coefficients $a_{1K} = 0.17 \pm 0.17$, $a_{2K} = 0.115 \pm 0.115$; $a_{1K^*} = 0.03 \pm 0.03$, $a_{2K^*} = 0.11 \pm 0.11$, respectively. Additionally, the final-state interactions remains unsettled in pQCD, which is non-perturbative but not universal. Fortunately, good agreement between the pQCD predictions for the branching ratios of $B \rightarrow KK$ decays [25] and currently available experimental measurements [24] indicates that the FSI effects are most possibly not important.

From the numerical results, it is easy to see that

- The pQCD predictions for the branching ratios of $B^+ \rightarrow K^+ \overline{K}^{*0}$ and $B^0 \rightarrow K^0 \overline{K}^{*0} + K^0 K^{*0}$ are consistent with currently available experimental upper limits. Inclusion of the NLO contributions decreases the central value of the LO predictions by about 30% to 80%. The chromo-magnetic penguin provide the dominant NLO contributions.
- For $B^0 \rightarrow K^+ K^{*-}$ decay, the pQCD prediction is rather different from that from the QCD factorization approach. Such difference could be tested in the forthcoming

LHCb experiments. For other decays, the pQCD predictions agree well with the corresponding QCDF results within one standard deviation.

C. CP-violating asymmetries

Now we turn to the evaluations of the CP-violating asymmetries of $B \rightarrow K^*K$ decays in pQCD approach. For $B^+ \rightarrow K^+\bar{K}^{*0}$ and $B^+ \rightarrow K^{*+}\bar{K}^0$ decays, the direct CP-violating asymmetries \mathcal{A}_{CP} can be defined as:

$$\mathcal{A}_{CP}^{dir} = \frac{|\overline{\mathcal{M}}_f|^2 - |\mathcal{M}_f|^2}{|\overline{\mathcal{M}}_f|^2 + |\mathcal{M}_f|^2}, \quad (76)$$

where $\mathcal{M}_f = \langle f | \mathcal{H}_{eff} | B \rangle$ and $\overline{\mathcal{M}}_f = \langle \bar{f} | \mathcal{H}_{eff} | B \rangle$.

The pQCD predictions for the direct CP-violating asymmetries of the considered decays are listed in Table III. For comparison, we also reproduce verbatim the corresponding numerical results evaluated in the framework of the QCD factorization (QCDF) [20].

TABLE III: The pQCD predictions for the direct CP asymmetries of $B \rightarrow KK^*$ decays (in units of percent).

Mode	LO	+VC	+QL	+MP	NLO	QCDF
$\mathcal{A}_{CP}^{dir}(B^+ \rightarrow K^+\bar{K}^{*0})$	-53.4	-39.2	-5.1	-49.8	-6.9	-24_{-39}^{+28}
$\mathcal{A}_{CP}^{dir}(B^+ \rightarrow K^{*+}\bar{K}^0)$	8.1	-12.3	7.2	10.6	6.5	-13_{-37}^{+29}

The pQCD predictions for \mathcal{A}_{CP}^{dir} and the major theoretical errors for $B^+ \rightarrow K^+\bar{K}^{*0}, K^{*+}\bar{K}^0$ decays are

$$\mathcal{A}_{CP}^{dir}(B^+ \rightarrow K^+\bar{K}^{*0}) = [-6.9_{-5.3}^{+5.6}(\omega_b)_{-0.3}^{+1.0}(\alpha)_{-6.5}^{+9.2}(a_{iK})_{-6.0}^{+4.0}(a_{iK^*})] \times 10^{-2}, \quad (77)$$

$$\mathcal{A}_{CP}^{dir}(B^+ \rightarrow K^{*+}\bar{K}^0) = [6.5_{-7.3}^{+7.9}(\omega_b)_{-1.4}^{+1.1}(\alpha)_{-7.7}^{+9.1}(a_{iK})_{-3.9}^{+2.1}(a_{iK^*})] \times 10^{-2}, \quad (78)$$

where the dominant errors come from the variations of $\omega_b = 0.4 \pm 0.04$ GeV, $\alpha = 100^\circ \pm 20^\circ$, and Gegenbauer coefficients $a_{1K} = 0.17 \pm 0.17$, $a_{2K} = 0.115 \pm 0.115$; $a_{1K^*} = 0.03 \pm 0.03$, $a_{2K^*} = 0.11 \pm 0.11$, respectively.

In Fig. 7, we show the α -dependence of the direct CP-violating asymmetries \mathcal{A}_{CP}^{dir} for $B^+ \rightarrow K^+\bar{K}^{*0}$ (the solid curve) and $B^+ \rightarrow K^{*+}\bar{K}^0$ (the dotted curve) decay, respectively. The left figure is for the LO pQCD predictions and the right one for the NLO pQCD predictions. One can see from the numbers and figures that (a) as usual, there exist relatively large differences between the pQCD and QCDF predictions; (b) the LO and NLO pQCD predictions for the direct CP-violating asymmetries are also rather different; and (c) the NLO contribution from the "Quark-loops" ("Vertex corrections") leads to the dominate change of \mathcal{A}_{CP}^{dir} for $B^+ \rightarrow K^+\bar{K}^{*0}$ ($B^+ \rightarrow K^{*+}\bar{K}^0$) decay.

We now study the CP-violating asymmetries for $B^0/\bar{B}^0 \rightarrow K^+K^{*-}(K^-K^{*+})$ decays. Since both B^0 and \bar{B}^0 can decay into the final state K^+K^{*-} and K^-K^{*+} , the four time-dependent decay widths for $B^0(t) \rightarrow K^+K^{*-}$, $\bar{B}^0(t) \rightarrow K^-K^{*+}$, $B^0(t) \rightarrow K^-K^{*+}$ and

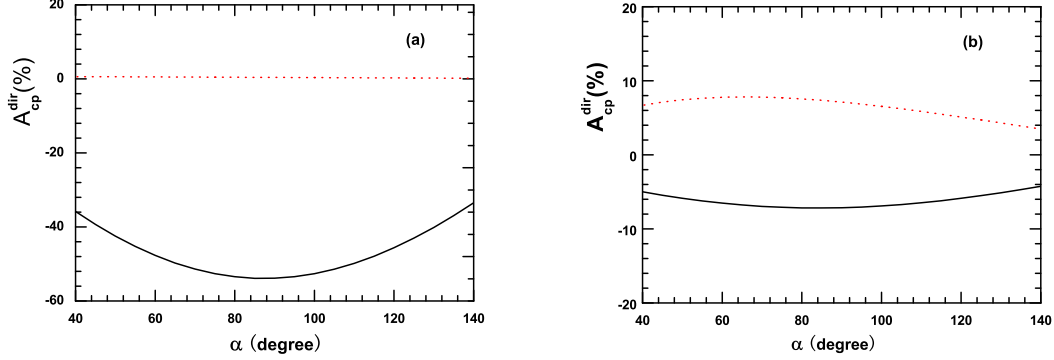


FIG. 7: The direct CP asymmetries (in percentage) of $B^+ \rightarrow K^+ \bar{K}^{*0}$ (solid curve) and $B^+ \rightarrow K^{*+} \bar{K}^0$ (dotted curve) as a function of CKM angle α . (a) shows the LO results, while (b) shows the NLO results.

$\bar{B}^0(t) \rightarrow K^+ K^{*-}$ can be expressed by four basic matrix elements:

$$\begin{aligned} g &= \langle K^+ K^{*-} | H_{eff} | B^0 \rangle, & h &= \langle K^+ K^{*-} | H_{eff} | \bar{B}^0 \rangle, \\ \bar{g} &= \langle K^- K^{*+} | H_{eff} | \bar{B}^0 \rangle, & \bar{h} &= \langle K^- K^{*+} | H_{eff} | B^0 \rangle, \end{aligned} \quad (79)$$

which determine the decay matrix elements of $B^0 \rightarrow K^+ K^{*-}$, $\bar{B}^0 \rightarrow K^- K^{*+}$, $B^0 \rightarrow K^- K^{*+}$ and $\bar{B}^0 \rightarrow K^+ K^{*-}$ at $t = 0$. Besides the matrix elements g, \bar{g}, h and \bar{h} , one also need to know the CP-violating parameter coming from the $B^0 - \bar{B}^0$ mixing:

$$B_1 = p|B^0\rangle + q|\bar{B}^0\rangle, \quad B_2 = p|B^0\rangle - q|\bar{B}^0\rangle, \quad (80)$$

with $|p|^2 + |q|^2 = 1$.

Following the notation of Ref. [10], the four time-dependent widths are given by the following formulae:

$$\begin{aligned} \Gamma(B^0(t) \rightarrow K^+ K^{*-}) &= e^{-\Gamma t} \frac{1}{2} (|g|^2 + |h|^2) \times \{1 + a_{\epsilon'} \cos(\Delta m t) + a_{\epsilon+\epsilon'} \sin(\Delta m t)\}, \\ \Gamma(\bar{B}^0(t) \rightarrow K^- K^{*+}) &= e^{-\Gamma t} \frac{1}{2} (|\bar{g}|^2 + |\bar{h}|^2) \times \{1 - a_{\bar{\epsilon}'} \cos(\Delta m t) - a_{\epsilon+\bar{\epsilon}'} \sin(\Delta m t)\}, \\ \Gamma(B^0(t) \rightarrow K^- K^{*+}) &= e^{-\Gamma t} \frac{1}{2} (|\bar{g}|^2 + |\bar{h}|^2) \times \{1 - a_{\bar{\epsilon}'} \cos(\Delta m t) - a_{\epsilon+\bar{\epsilon}'} \sin(\Delta m t)\}, \\ \Gamma(\bar{B}^0(t) \rightarrow K^+ K^{*-}) &= e^{-\Gamma t} \frac{1}{2} (|g|^2 + |h|^2) \times \{1 + a_{\epsilon'} \cos(\Delta m t) + a_{\epsilon+\epsilon'} \sin(\Delta m t)\}, \end{aligned} \quad (81)$$

where the CP -violating parameters are

$$\begin{aligned} a_{\epsilon'} &= \frac{|g|^2 - |h|^2}{|g|^2 + |h|^2}, & a_{\epsilon+\epsilon'} &= \frac{-2\text{Im}(\frac{q}{p} \frac{h}{g})}{1 + |h/g|^2} \\ a_{\bar{\epsilon}'} &= \frac{|\bar{h}|^2 - |\bar{g}|^2}{|\bar{h}|^2 + |\bar{g}|^2}, & a_{\epsilon+\bar{\epsilon}'} &= \frac{-2\text{Im}(\frac{q}{p} \frac{\bar{g}}{\bar{h}})}{1 + |\bar{g}/\bar{h}|^2}, \end{aligned} \quad (82)$$

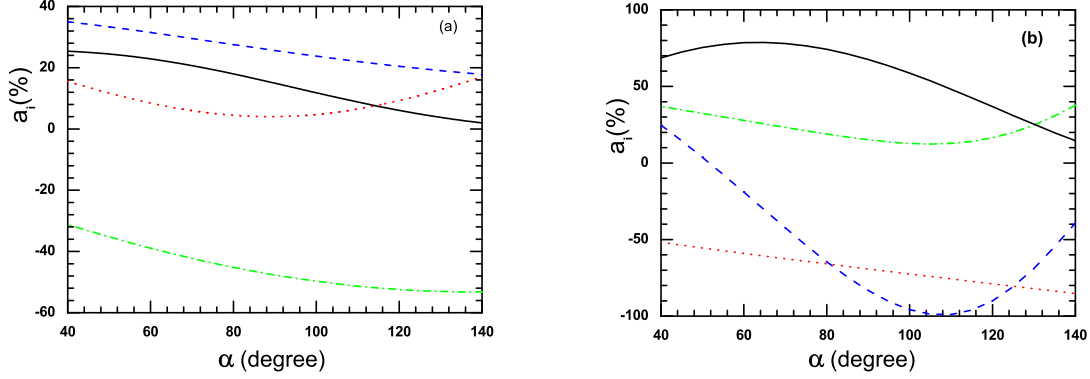


FIG. 8: The CP-violating parameters of $B^0/\bar{B}^0 \rightarrow K^0\bar{K}^{*0}$ ($K^0 K^{*0}$) decays, (a); and $B^0/\bar{B}^0 \rightarrow K^+ K^{*-}$ ($K^- K^{*+}$) decays, (b) : $a_{e'}$ (dash-dotted line), $a_{\bar{e}'}$ (dotted line), $a_{e+e'}$ (dashed line) and $a_{e+\bar{e}'}$ (solid line) as a function of CKM angle α .

with $q/p = e^{-2i\beta}$ and $\beta = 21.6^\circ$ is one of the three CKM angles.

Similarly, the four time-dependent decay widths for $B^0 \rightarrow K^0\bar{K}^{*0}$, $\bar{B}^0 \rightarrow K^0\bar{K}^{*0}$, $B^0 \rightarrow \bar{K}^0 K^{*0}$ and $\bar{B}^0 \rightarrow \bar{K}^0 K^{*0}$ (here K^0 means K_S^0) can also be defined as

$$\begin{aligned} g &= \langle K^0\bar{K}^{*0} | H_{eff} | B^0 \rangle, & h &= \langle K^0\bar{K}^{*0} | H_{eff} | \bar{B}^0 \rangle, \\ \bar{g} &= \langle \bar{K}^0 K^{*0} | H_{eff} | \bar{B}^0 \rangle, & \bar{h} &= \langle \bar{K}^0 K^{*0} | H_{eff} | B^0 \rangle, \end{aligned} \quad (83)$$

One can define, consequently, the four CP-violating parameters $a_{e'}$, $a_{e+e'}$, $a_{\bar{e}'}$ and $a_{e+\bar{e}'}$ for $B^0/\bar{B}^0 \rightarrow f_1 + \bar{f}_1$ decays in the same way as in Eq. (82). In Fig. 8, we show the pQCD predictions for the eight CP-violating parameters for the considered decays.

The central values of the pQCD predictions for the CP-violating parameters are

$$a_{e'} = 0.13, \quad a_{e+e'} = -0.96, \quad a_{\bar{e}'} = -0.72, \quad a_{e+\bar{e}'} = 0.59. \quad (84)$$

for $B^0/\bar{B}^0 \rightarrow K^+ K^{*-} + K^- K^{*+}$ decays, and

$$a_{e'} = -0.50, \quad a_{e+e'} = 0.24, \quad a_{\bar{e}'} = 0.05, \quad a_{e+\bar{e}'} = 0.12, \quad (85)$$

for $B^0/\bar{B}^0 \rightarrow K^0\bar{K}^{*0} + \bar{K}^0 K^{*0}$ decays.

As pointed in Ref. [26], it may be conceptually incorrect to evaluate the Wilson coefficients at scales down to 0.5 GeV. The explicit numerical values for the Wilson coefficients $C_1(\mu) - C_{10}(\mu)$ for $\mu = 0.5, 1.0, 1.5$ and 2.0 GeV, as listed in Table IV, also support this expectation: the values of the Wilson coefficients $C_{3,4,5,6}(\mu)$ at $\mu = 0.5$ GeV are about four to seven times larger than those at $\mu = 1.0$ GeV. For $C_5(\mu)$, specifically, $C_5(0.5)$ and $C_5(1.0)$ even have a different sign besides the large difference in their magnitude. In the region of $\mu \geq 1.0$ GeV, however, the μ -dependence of all Wilson coefficients become relatively weak. It is therefore reasonable for us to choose $\mu_0 = 1.0$ GeV as the lower

cut-off of the hard scale, instead of $\mu_0 = 0.5$ GeV as being assumed in Ref. [13]. We then fix the values $C_i(\mu)$ at $C_i(\mu_0 = 1.0)$, whenever the scale μ runs to below the scale μ_0 .

In order to show directly the μ_0 -dependence of the branching ratios and CP-violating asymmetries, we recalculated these quantities for $B \rightarrow KK^*$ decays by setting $\mu_0 = 0.5, 1.0, 1.5$ and 2.0 GeV, respectively. It is easy to see from the numerical results as listed in Table V that the pQCD predictions are relatively stable against the variation of μ_0 for $\mu_0 \geq 1.0$ GeV. We therefore set $\mu_0 = 1.0$ GeV to be the cut-off scale for Wilson coefficients $C_i(\mu)$. Of course, the issue of μ_0 -dependence need more studies.

TABLE IV: NLO Wilson coefficients $C_i(\mu)$ for $\mu_0 = 0.5 - 2.0$ GeV, respectively.

μ_0	$C_1(\mu)$	$C_2(\mu)$	$C_3(\mu)$	$C_4(\mu)$	$C_5(\mu)$	$C_6(\mu)$	$C_7(\mu)$	$C_8(\mu)$	$C_9(\mu)$	$C_{10}(\mu)$
0.5 GeV	-0.9923	1.6537	0.1729	-0.3122	-0.1143	-0.8276	0.0010	0.0056	-0.0148	0.0092
1.0 GeV	-0.5093	1.2790	0.0428	-0.0898	0.0150	-0.1321	-0.0002	0.0008	-0.0120	0.0050
1.5 GeV	-0.3773	1.1920	0.0289	-0.0652	0.0153	-0.0856	-0.0002	0.0005	-0.0112	0.0038
2.0 GeV	-0.3114	1.1518	0.0230	-0.0541	0.0145	-0.0672	-0.0002	0.0004	-0.0108	0.0032

TABLE V: The pQCD predictions for the branching ratios (in unit of 10^{-7}) and direct CP-violating asymmetries (in unit of 10^{-2}) for the considered $B \rightarrow KK^*$ decays, assuming $\mu_0 = 0.5, 1.0, 1.5$ and 2.0 GeV, respectively.

Mode	$\mu_0 = 0.5$	$\mu_0 = 1.0$	$\mu_0 = 1.5$	$\mu_0 = 2.0$
$Br(B^+ \rightarrow K^+ \bar{K}^{*0})$	4.7	3.2	2.6	2.1
$Br(B^+ \rightarrow K^{*+} \bar{K}^0)$	2.6	2.1	1.3	0.8
$Br(B^0/\bar{B}^0 \rightarrow f_1 + \bar{f}_1)$	22.5	8.5	5.0	3.5
$Br(B^0/\bar{B}^0 \rightarrow f_2 + \bar{f}_2)$	5.4	1.3	0.78	0.55
$\mathcal{A}_{CP}^{dir}(B^+ \rightarrow K^+ \bar{K}^{*0})$	-4.0	-6.9	-7.1	-5.1
$\mathcal{A}_{CP}^{dir}(B^+ \rightarrow K^{*+} \bar{K}^0)$	16.8	6.5	-1.5	-5.8

VI. SUMMARY

In this paper, we calculate some NLO contributions to the branching ratios and CP-violating asymmetries of $B \rightarrow KK^*$ decays in the pQCD factorization approach.

From our calculations and phenomenological analysis, we found the following results:

- The NLO contributions from the QCD vertex corrections, the quark-loops and the chromo-magnetic penguins can be rather large and provide significant modifications to the LO predictions.

- The NLO pQCD predictions for the form factors of $B \rightarrow K^*$ and K transitions are

$$\begin{aligned} A_0^{B \rightarrow K^*}(q^2 = 0) &= 0.38 \pm 0.05(\omega_b), \\ F_{0,1}^{B \rightarrow K}(q^2 = 0) &= 0.36 \pm 0.06(\omega_b), \end{aligned} \quad (86)$$

for $\omega_b = 0.40 \pm 0.04 \text{ GeV}$, which agree well with those obtained in QCD sum rule calculations.

- The pQCD predictions for the branching ratios are

$$\begin{aligned} Br(B^+ \rightarrow \bar{K}^{*0} K^+) &= 3.2_{-0.8}^{+1.2} \times 10^{-7}, \\ Br(B^+ \rightarrow K^{*+} \bar{K}^0) &= 2.1_{-1.2}^{+1.4} \times 10^{-7}, \\ Br(B^0 \rightarrow K^0 \bar{K}^{*0} + \bar{K}^0 K^{*0}) &= 8.5_{-2.1}^{+2.6} \times 10^{-7}, \\ Br(B^0 \rightarrow K^+ K^{*-} + K^- K^{*+}) &= 1.3_{-0.7}^{+0.5} \times 10^{-7}, \end{aligned} \quad (87)$$

where the theoretical errors from various sources are added in quadrature. These pQCD predictions are consistent with both the QCDF predictions and currently available experimental upper limits.

- The direct CP-violating asymmetries for $B^+ \rightarrow K^+ \bar{K}^{*0}$, $K^{*+} \bar{K}^0$ are (in unit of 10^{-2})

$$\begin{aligned} \mathcal{A}_{CP}^{dir}(B^+ \rightarrow K^+ \bar{K}^{*0}) &= -6.9_{-10.3}^{+11.5}, \\ \mathcal{A}_{CP}^{dir}(B^+ \rightarrow K^{*+} \bar{K}^0) &= 6.5_{-11.4}^{+12.3}, \end{aligned} \quad (88)$$

which are rather different from those in the QCDF approach.

Acknowledgments

The authors are very grateful to Hsiang-nan Li, Cai-Dian Lü, Ying Li, Wei Wang and Yu-Ming Wang for helpful discussions. This work is partly supported by the National Natural Science Foundation of China under Grant No.10575052 and 10735080.

APPENDIX A: RELATED FUNCTIONS

We show here the function h_i 's, coming from the Fourier transformations of $H^{(0)}$,

$$\begin{aligned} h_e(x_1, x_2, b_1, b_2) &= K_0(\sqrt{x_1 x_2} m_B b_1) [\theta(b_1 - b_2) K_0(\sqrt{x_2} m_B b_1) I_0(\sqrt{x_2} m_B b_2) \\ &\quad + \theta(b_2 - b_1) K_0(\sqrt{x_2} m_B b_2) I_0(\sqrt{x_2} m_B b_1)] S_t(x_2), \end{aligned} \quad (A1)$$

$$\begin{aligned} h_a(x_2, x_3, b_2, b_3) &= K_0\left(i\sqrt{(1-x_2)x_3} m_B b_2\right) [\theta(b_3 - b_2) K_0(i\sqrt{x_3} m_B b_3) I_0(i\sqrt{x_3} m_B b_2) \\ &\quad + \theta(b_2 - b_3) K_0(i\sqrt{x_3} m_B b_2) I_0(i\sqrt{x_3} m_B b_3)] S_t(x_3), \end{aligned} \quad (A2)$$

$$\begin{aligned}
h_f(x_1, x_2, x_3, b_1, b_3) = & \left\{ \theta(b_1 - b_3) K_0(m_B \sqrt{x_1 x_2} b_1) I_0(m_B \sqrt{x_1 x_2} b_3) \right. \\
& \left. + \theta(b_3 - b_1) K_0(m_B \sqrt{x_1 x_2} b_3) I_0(m_B \sqrt{x_1 x_2} b_1) \right\} \\
& \cdot \left(\begin{array}{l} \frac{\pi i}{2} H_0(\sqrt{(x_2(x_3 - x_1))} m_B b_3), \text{ for } x_1 - x_3 < 0 \\ K_0^{(1)}(\sqrt{(x_2(x_1 - x_3))} m_B b_3), \text{ for } x_1 - x_3 > 0 \end{array} \right), \quad (\text{A3})
\end{aligned}$$

$$\begin{aligned}
h_f^3(x_1, x_2, x_3, b_1, b_3) = & \left\{ \theta(b_1 - b_3) K_0(i\sqrt{(1-x_2)x_3} b_1 M_m) I_0(i\sqrt{(1-x_2)x_3} b_3 m_B) \right. \\
& \left. + (\theta(b_3 - b_1) K_0(i\sqrt{(1-x_2)x_3} b_3 m_B) I_0(i\sqrt{(1-x_2)x_3} b_1 m_B)) \right\} \\
& \cdot \left(\begin{array}{l} K_0(m_B \sqrt{(x_1 - x_3)(1-x_2)} b_1), \text{ for } x_1 - x_3 > 0 \\ \frac{\pi i}{2} H_0^{(1)}(m_B \sqrt{(x_3 - x_1)(1-x_2)} b_1), \text{ for } x_1 - x_3 < 0 \end{array} \right), \quad (\text{A4})
\end{aligned}$$

$$\begin{aligned}
h_f^4(x_1, x_2, x_3, b_1, b_2) = & \left\{ \theta(b_1 - b_3) K_0(i\sqrt{(1-x_2)x_3} b_1 m_B) I_0(i\sqrt{(1-x_2)x_3} b_3 m_B) \right. \\
& \left. + \theta(b_3 - b_1) K_0(i\sqrt{(1-x_2)x_3} b_3 m_B) I_0(i\sqrt{(1-x_2)x_3} b_1 m_B) \right\} \\
& \cdot \left(\begin{array}{l} K_0(m_B F_1 b_1), \text{ for } F_1^2 > 0 \\ \frac{\pi i}{2} H_0^{(1)}(m_B \sqrt{|F_1^2|} b_1), \text{ for } F_1^2 < 0 \end{array} \right), \quad (\text{A5})
\end{aligned}$$

where J_0 is the Bessel function and K_0 , I_0 are modified Bessel functions $K_0(-ix) = -(\pi/2)Y_0(x) + i(\pi/2)J_0(x)$, and $F_{(1)}$'s are defined by

$$F_{(1)}^2 = 1 - x_2(1 - x_3 - x_1). \quad (\text{A6})$$

The threshold resummation form factor $S_t(x_i)$ is adopted from Ref.[27]. It has been parametrized as

$$S_t(x) = \frac{2^{1+2c} \Gamma(3/2 + c)}{\sqrt{\pi} \Gamma(1 + c)} [x(1-x)]^c, \quad (\text{A7})$$

where the parameter $c = 0.3$.

The evolution factors $E_e^{(l)}$ and $E_a^{(l)}$ appeared in Eqs. (19) to (38) are given by

$$\begin{aligned}
E_e(t) &= \alpha_s(t) \exp[-S_{ab}(t)], \\
E_e'(t) &= \alpha_s(t) \exp[-S_{cd}(t)]|_{b_2=b_1}, \\
E_a(t) &= \alpha_s(t) \exp[-S_{gh}(t)], \\
E_a'(t) &= \alpha_s(t) \exp[-S_{ef}(t)]|_{b_2=b_3}, \quad (\text{A8})
\end{aligned}$$

where the Sudakov factors can be written as

$$S_{ab}(t) = s\left(x_1 m_B/\sqrt{2}, b_1\right) + s\left(x_2 m_B/\sqrt{2}, b_2\right) + s\left((1-x_2)m_B/\sqrt{2}, b_2\right) - \frac{1}{\beta_1} \left[\ln \frac{\ln(t/\Lambda)}{-\ln(b_1\Lambda)} + \ln \frac{\ln(t/\Lambda)}{-\ln(b_2\Lambda)} \right], \quad (\text{A9})$$

$$S_{cd}(t) = s\left(x_1 m_B/\sqrt{2}, b_1\right) + s\left(x_2 m_B/\sqrt{2}, b_1\right) + s\left((1-x_2)m_B/\sqrt{2}, b_1\right) + s\left(x_3 m_B/\sqrt{2}, b_3\right) + s\left((1-x_3)m_B/\sqrt{2}, b_3\right) - \frac{1}{\beta_1} \left[2 \ln \frac{\ln(t/\Lambda)}{-\ln(b_1\Lambda)} + \ln \frac{\ln(t/\Lambda)}{-\ln(b_3\Lambda)} \right], \quad (\text{A10})$$

$$S_{ef}(t) = s\left(x_1 m_B/\sqrt{2}, b_1\right) + s\left(x_2 m_B/\sqrt{2}, b_2\right) + s\left((1-x_2)m_B/\sqrt{2}, b_2\right) + s\left(x_3 m_B/\sqrt{2}, b_2\right) + s\left((1-x_3)m_B/\sqrt{2}, b_2\right) - \frac{1}{\beta_1} \left[\ln \frac{\ln(t/\Lambda)}{-\ln(b_1\Lambda)} + 2 \ln \frac{\ln(t/\Lambda)}{-\ln(b_2\Lambda)} \right], \quad (\text{A11})$$

$$S_{gh}(t) = s\left(x_2 m_B/\sqrt{2}, b_2\right) + s\left(x_3 m_B/\sqrt{2}, b_3\right) + s\left((1-x_2)m_B/\sqrt{2}, b_2\right) + s\left((1-x_3)m_B/\sqrt{2}, b_3\right) - \frac{1}{\beta_1} \left[\ln \frac{\ln(t/\Lambda)}{-\ln(b_1\Lambda)} + \ln \frac{\ln(t/\Lambda)}{-\ln(b_2\Lambda)} \right], \quad (\text{A12})$$

where the function $s(q, b)$ are defined in the Appendix A of Ref.[6].

The hard scale t_i 's appeared in Eqs. (19) to (38) are of the form

$$t_a = \max(\sqrt{x_2}m_B, \sqrt{x_1 x_2}m_B, 1/b_1, 1/b_2), \quad t'_a = \max(\sqrt{x_1}m_B, \sqrt{x_1 x_2}m_B, 1/b_1, 1/b_2), \quad (\text{A13})$$

$$t_b = \max(\sqrt{x_2|1-x_3-x_1|}m_B, \sqrt{x_1 x_2}m_B, 1/b_1, 1/b_3), \quad t'_b = \max(\sqrt{x_2|x_3-x_1|}m_B, \sqrt{x_1 x_2}m_B, 1/b_1, 1/b_3), \quad (\text{A14})$$

$$t_c = \max(\sqrt{(1-x_2)x_3}m_B, \sqrt{|x_1-x_3|(1-x_2)}m_B, 1/b_1, 1/b_3), \quad t'_c = \max(\sqrt{|1-x_2(1-x_3-x_1)|}m_B, \sqrt{(1-x_2)x_3}m_B, 1/b_1, 1/b_3), \quad (\text{A15})$$

$$t_d = \max(\sqrt{(1-x_2)x_3}m_B, \sqrt{(1-x_2)}m_B, 1/b_2, 1/b_3), \quad t'_d = \max(\sqrt{(1-x_2)x_3}m_B, \sqrt{x_3}m_B, 1/b_2, 1/b_3). \quad (\text{A16})$$

-
- [1] I.I. Bigi and A.I. Sanda, *CP Violation* (Cambridge University Press, Cambridge, England, 2000); G.C. Branco, L. Lavoura and J.P. Silva, *CP Violation* (Oxford University Press, Oxford, England, 1999);
- [2] H.-n. Li, Prog. Part. & Nucl. Phys. **51**, 85 (2003) and references therein.
- [3] M. Beneke, G. Buchalla, M. Neubert, and C.T. Sachrajda, Phys. Rev. Lett. **83**, 1914 (1999); Nucl. Phys. B **591**, 313 (2000).

- [4] C.W.Bauer, D.Pirjol, I.Z. Rothstein and I.W. Stewart, Phys. Rev. D **70**, 054015 (2004); M. Beneke and T. Feldmann, Nucl. Phys. B **685**, 249(2004).
- [5] Y.-Y. Keum, H.-n. Li and A.I. Sanda, Phys. Rev. D **63**, 054008 (2001).
- [6] C.D. Lü, K. Ukai and M.Z. Yang, Phys. Rev. D **63**, 074009 (2001).
- [7] H.-n. Li, Phys. Rev. D **64**, 014019 (2001); C.-H. Chen, Y.-Y. Keum, and H.-n. Li, Phys. Rev. D **64**,112002 (2001); Phys. Rev. D **66**,054013 (2002); Y.-Y. Keum and A.I. Sanda, Phys. Rev. D **67**, 054009 (2003).
- [8] Y. Li, C.D. Lü, Z.J. Xiao, and X.Q. Yu, Phys. Rev. D **70**, 034009 (2004); Y. Li, C.D. Lü, and Z.J. Xiao, J. Phys. G **31**, 273 (2005).
- [9] X. Liu, H.S. Wang, Z.J. Xiao, L.B. Guo, and C.D. Lü, Phys. Rev. D **73**, 074002 (2006); H.S. Wang, X. Liu, Z.J. Xiao, L.B. Guo, and C.D. Lü, Nucl. Phys. B **738**, 243 (2006).
- [10] L.B. Guo, Q.G. Xu and Z.J. Xiao, Phys. Rev. D **75**, 014019 (2007).
- [11] A. Ali, G. Kramer, Y. Li, C.D. Lü, Y.L. Shen, W. Wang and Y.M. Wang, Phys. Rev. D **76**, 014008 (2007).
- [12] Z.J. Xiao, X.F. Chen and D.Q. Guo, Eur. Phys. J. C **50**, 363 (2007); Z.J. Xiao, X. Liu and H.S. Wang, Phys. Rev. D **75**, 034017 (2007).
- [13] H.-n. Li, S. Mishima, A.I. Sanda, Phys. Rev. D **72**, 114005 (2005).
- [14] H.-n. Li, S. Mishima, Phys. Rev. D **74**, 094020 (2006).
- [15] H.-n. Li, Phys. Rev. D **66**, 094010 (2002).
- [16] G. Buchalla, A.J. Buras, and M.E. Lautenbacher, Rev. Mod. Phys. **68**, 1125 (1996).
- [17] C.D. Lü, M.Z. Yang, Eur. Phys. J. C **28**, 515 (2003).
- [18] P. Ball, V.M. Braun, Y. Koike, and K. Tanaka, Nucl. Phys. B **529**, 323 (1998); P. Ball, J. High Energy Phys. **09** (1998) 005.
- [19] P. Ball and R. Zwicky, Phys. Rev. D **71**, 014015 (2005); J. High Energy Phys. **04** (2006) 046.
- [20] M. Beneke and M. Neubert, Nucl. Phys. B **675**, 333 (2003).
- [21] M. Bander, D. Silverman and A. Soni, Phys. Rev. Lett. **43**, 242 (1979); J.M. Jerard and W.S. Hou, Phys. Rev. D **43**, 2909 (1991);
- [22] S. Mishima and A.I. Sanda, Prog. Theor. Phys. **110**, 549 (2003).
- [23] Particle Data Group, W.-M. Yao *et al.*, J. Phys. G **33**, 1 (2006).
- [24] E. Barberio *et al.*, (Heavy Flavor Averaging Group), hep-ex/0704.3575; for update see: <http://www.slac.stanford.edu/xorg/hfag>.
- [25] C.-h. Chen and H.-n. Li, Phys. Rev. D **63**, 014003 (2000); C.D. Lü, Y.L. Shen and W. Wang, Phys. Rev. D **73**, 034005 (2006).
- [26] M. Beneke, Nucl.Phys.B(Proc.Suppl.) **170**, 57 (2007).
- [27] T. Kurimoto, H.-n. Li, A.I. Sanda, Phys. Rev. D **65**, 014007 (2002).